5th INTERNATIONAL MAAR CONFERENCE

The Valle de Santiago maars, México: the record of magma-water fluctuations during the formation of a basaltic maar (La Alberca) and active post-desiccation subsidence at the bottom of a maar lake (Rincón de Parangueo)

Intra-conference Field trip
5th International Maar Conference, Querétaro, México

José Jorge Aranda-Gómez and Gerardo Carrasco-Núñez

Centro de Geociencias, Universidad Nacional autónoma de México,
UNAM Campus Juriquilla, Querétaro, Qro., 76100 México.

November 20th, 2014

http://maar2014.geociencias.unam.mx

Cover description: Northern wall of La Alberca crater as seen in August 2010. Note that the small “playa-lake” has a slight red color, probably due to the presence of a cyanobacteria bloom in the water. Photo by: José Jorge Aranda-Gómez.

Universidad Nacional Autónoma de México
Centro de Geociencias

Querétaro, Mexico,
November 2014

Edition and design:
J. Jesús Silva Corona

The Valle de Santiago maars, México: the record of magma-water fluctuations during the formation of a basaltic maar (La Alberca) and active post-desiccation subsidence at the bottom of a maar lake (Rincón de Parangueo)

Jóse Jorge Aranda-Gómez* and Gerardo Carrasco-Núñez**

[1] Centro de Geociencias, Universidad Nacional autónoma de México, UNAM Campus Juriquilla, Querétaro, Qro., 76100 México.
** jjag@geociencias.unam.mx, **gerardoc@geociencias.unam.mx*

PART I: OVERVIEW

Purpose and scope

This one-day field trip is devoted to show to the attendees of the 5IMC some of the main volcanological characteristics of Valle de Santiago maars, as exemplified by La Alberca Maar, and to discuss some intriguing changes that are actively occurring inside the crater of the Rincón de Parangueo maar. At least four of the maars around Valle de Santiago (La Alberca, Rincón de Parangueo, Cíntora and San Nicolás) hosted perennial lakes in the early 1900's (Ordóñez, 1900), as all these crater-lakes were in part fed by groundwater. Now, they are all dry, because they were gradually desiccated in the past decades. This phenomenon began during the 1980's as a consequence of drawdown in the Valle de Santiago – Salamanca aquifer.

Land subsidence and formation of aseismic faults is commonly associated with drawdown in confined and semi-confined aquifers throughout the extensive plain located between Querétaro and Valle de Santiago (El Bajío, Figure 1). There are a large number of wells pumping out groundwater to sustain intensive agriculture and a growing industry and population in El Bajío. Land subsidence and associated "faulting" has been documented in several cities located in El Bajío, such as Celaya, Salamanca, Irapuato and Silao (Figure 1). However, subsidence-related faults also

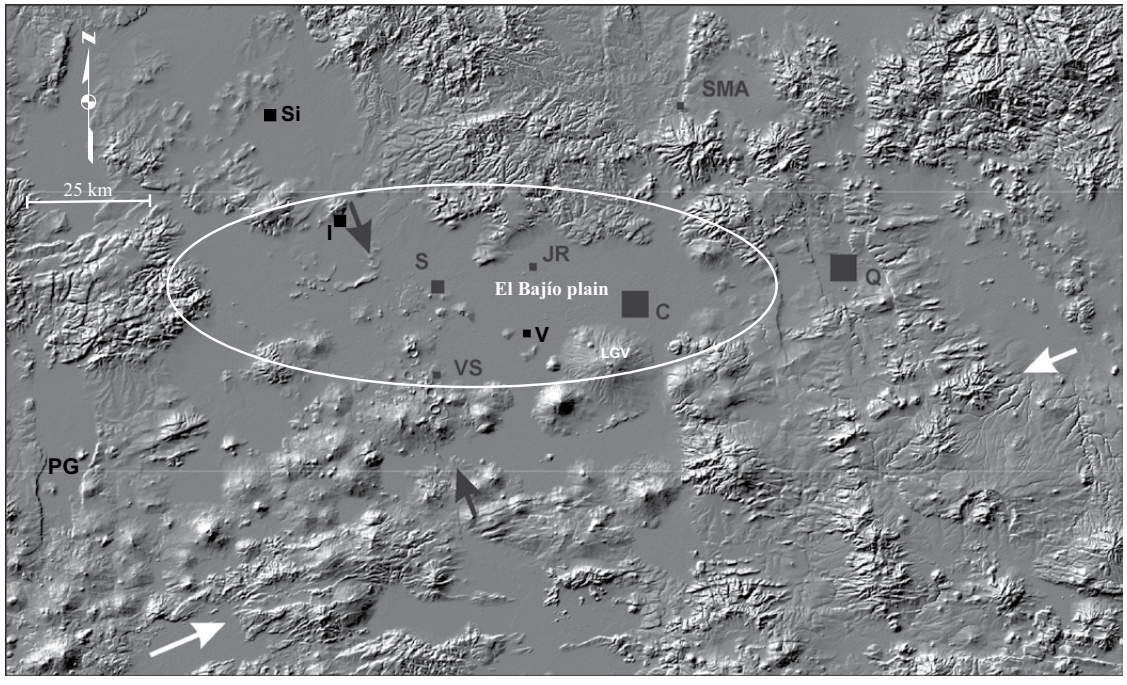

Figure 1. El Bajío region and its surroundings shown in a DEM. Black arrows point out the N25W-trending maar lineament where La Alberca and Rincón de Parangueo are located; white arrows signal the Chapala rift trend (N80E). Note that the NNW-trending faults of the Taxco – San Miguel Allende fault system are well exposed in the Querétaro area. Subsidence related faults in Querétaro and Celaya are roughly parallel to the Taxco – San Miguel Allende fault system, whereas the Salamanca faults follow the Chapala graben trend. Near the SW corner of the figure is the Penjamillo Graben (PG). Key to localities mentioned in the text: A= Abasolo, C = Celaya, Co= Cortazar, I = Irapuato, JR = Juventino Rosas, Q = Querétaro S = Salamanaca, SMA = San Miguel Allende, Si = Silao, V = Villagrán and VS = Valle de Santiago (Aranda-Gómez *et al.*, 2013).

exist in rural areas, as it can be seen on the paved road between Juventino Rosas and Villagrán (Figure 1). The land subsidence-related fault nearest to the Valle de Santiago maars is located in Salamanca (Borja-Ortíz y Rodríguez, 2004), 14 km NNW of the center of the Rincón de Parangueo maar.

In a study of the water chemistry of 15 crater lakes throughout Mexico Armienta *et al.*(2008) found that the most extreme values (ion concentrations, pH = 10.2, and conductivity > 165,000 µS/cm) occurring the highly evaporated residual waters at Rincón de Parangueo, one of volcanoes visited in this field trip. We reported the presence of evaporites near the remnants of the lake.

A large number of deformation features can be observed on the surface of the desiccated lake bed inside the crater of Rincón de Parangueo; the most remarkable structure is a topographic scarp, on the average 10 -12 m high, which was produced by a segmented normal fault with an annular shape, which formed around the lake depocenter. The fault system is located near the former lake shore. It has been argued that that topographic scarp reflects the original bathymetry at the bottom of the crater-lake (*e.g.* Escolero-Fuentes y Alcocer-Durand, 2004) or that the scarp was produced by the deformation and subaqueous landslides produced during the 8.1 magnitude earthquake of September 19, 1985 (Kienle *et al.*, 2009). As opposed to these interpretations about the origin of the scarp, we believe that this feature is the product of local accelerated subsidence, which probably began prior to the final lake desiccation and it is a consequence of:

1. Progressive compaction of the lake sediments and a diatreme located below the maar crater, and/or
2. Dissolution and removal of evaporites (trona: $Na_3H(CO_3)_2 \cdot 2H_2O$; thermonatrite [$Na_2CO_3$ *H_2O], natrite [Na_2CO_3], eitelite [$Na_2Mg(CO_3)_2$], halite [NaCl], sylvite: [KCl], which are present in the lake sediments, specially close to the remaining vestiges of the original lake, and/or
3. Land subsidence, as it is observed in other parts of the Valle de Santiago – Salamanca aquifer.

Independently of the origin of the ring fault and as a consequence of local conditions such as: (1) the size and curvature of the annular fault, and (2) the occurrence of finely laminated mudstones, which are dry-on-the-surface and water-saturated at depth, the topographic scarp is the ideal place to observe and interpret active subsidence-related deformation, the development of rotational landslides and associated structures, and the growth of structural domes caused by "mud tectonics". Compared with other localities in El Bajío region where "subsidence-creep-fault processes" (Ávila-Olivera *et al.*, 2008) are occurring, displacement rate at the Rincón de Parangueo annular fault is at least one order of magnitude larger. Thus, in Rincón de Parangueo is the opportunity to document the progressive changes caused by subsidence and gradual steepening of the terrain.

Finally, the lakes inside La Alberca and Rincón de Parangueo sustained colonies of stromatolites, which are "organo sedimentary structures produced by sediment trapping, binding and/or precipitation as a result of the growth and metabolic activity of microorganisms…" (Walter, 1976). In the case of Rincón de Parangueo´s stromatolites, they are made of calcium and magnesium carbonates. Modern stromatolites are living examples of one of the Earth's oldest and most persistent widespread ecosystems. Some of these organisms are considered extremophiles, as they thrive in geochemical extreme conditions such as those found in Rincón de Parangueo.

This guidebook is a follow-up and builds on two previous guidebooks and a recently published paper (Aranda-Gómez *et al.*, 2013). One of the guidebooks was associated to a one-day field trip held during WRI-13 (Aranda-Gómez *et al.*, 2010a), and the other to a two-day field trip held during EISOLS meeting (Aranda-Gómez *et al.*, 2010b). Large portions of text of the introductory part were extracted from those unpublished documents. However, emphasis in the WRI guidebook was centered on the extreme salinity of the water inside Rincón de Parangueo, as compared with the rest of the regional aquifer. In addition to this topic, the EISOLS field trip and the 2013 paper focused on land subsidence related to drawdown in two (?) aquifers at El Bajío region and on the large contrast in the morphology of the dry lake beds in the recently desiccated crater-lakes around Valle de Santiago. As we will see in this 2014 version of the field trip, La Alberca crater shows on its walls clear evidence of the desiccation process, as the highest water stand is evidenced by nearly white stromatolites that grew on the vertical pre-maar lavas exposed on the crater's walls. Height difference between the stromatolite marker line and the dry bottom of the former lake together with the time lapse needed to accomplish desiccation can be used to make a quick calculation of the drawdown rate in the aquifer (about 2 m/year: Escolero-Fuentes and Alcocer-Durand, 2004). The bottom of La Alberca displays the characteristic morphology shown by these lakes after desiccation and permits to make a comparison with the strikingly different morphology of Rincón de Parangueo, where rapid subsidence has occurred in the past 35 years and it is still active.

Most of our visit to Rincón de Parangueo will be devoted to study the deformation features along the ring fault and at the subsided portion of the lake bed, near the base of the topographic scarp. We will also see structural evidence of soluble salts removal from the interior of the crater. This, we believe, was accomplished by rainwater, which dissolved the evaporites, and later, by infiltration of highly concentrated brine towards the aquifer. The end result of this process, combined with compaction of the lake sediments and the underlying diatreme is an unusually high subsidence rate in this particular maar.

Introduction: phreatomagmatic activity and the Valle de Santiago volcanic field

The phreatomagmatic volcanoes of Valle de Santiago are located at the northern end of the Michoacán-Guanajuato volcanic field (MGVF; Figure 2), a vast region (nearly 40,000 km²) with more than 1000 monogenetic volcanoes (Hasenaka and Carmichael, 1985), which is located in the central part of the Trans Mexican Volcanic Belt (TMVB). Magmatic activity at the TMVB is mostly produced by subduction of the Rivera and Cocos plates underneath the North American plate along the Middle American Trench (Figures 1 and 2). Therefore, most volcanoes in the TMVB are calc-alkaline (Luhr *et al.*, 2006). However, small volumes of intra-plate mafic alkaline rocks are also found in many localities in the TMVB, reflecting the involvement of a different magma source akin to the magma source in the mantle that is feeding the intra-plate volcanoes in the Mexican Extensional Province (Luhr *et al.*, 2006), which is located north of the TMVB. Chemical composition of the volcanic products of the Valle de Santiago area, suggest that an additional component to the calc-alkaline magmas is present in the genesis of some of the young volcanoes in the region. While some rocks have a clear subduction signature, others have chemical compositions that resemble those of the alkaline intra-plate lavas of the Mexican Extensional Province located immediately north of Valle de Santiago. Furthermore, some of the volcanoes in the Valle de Santiago region were formed by megacryst- and/or feldspathic granu-

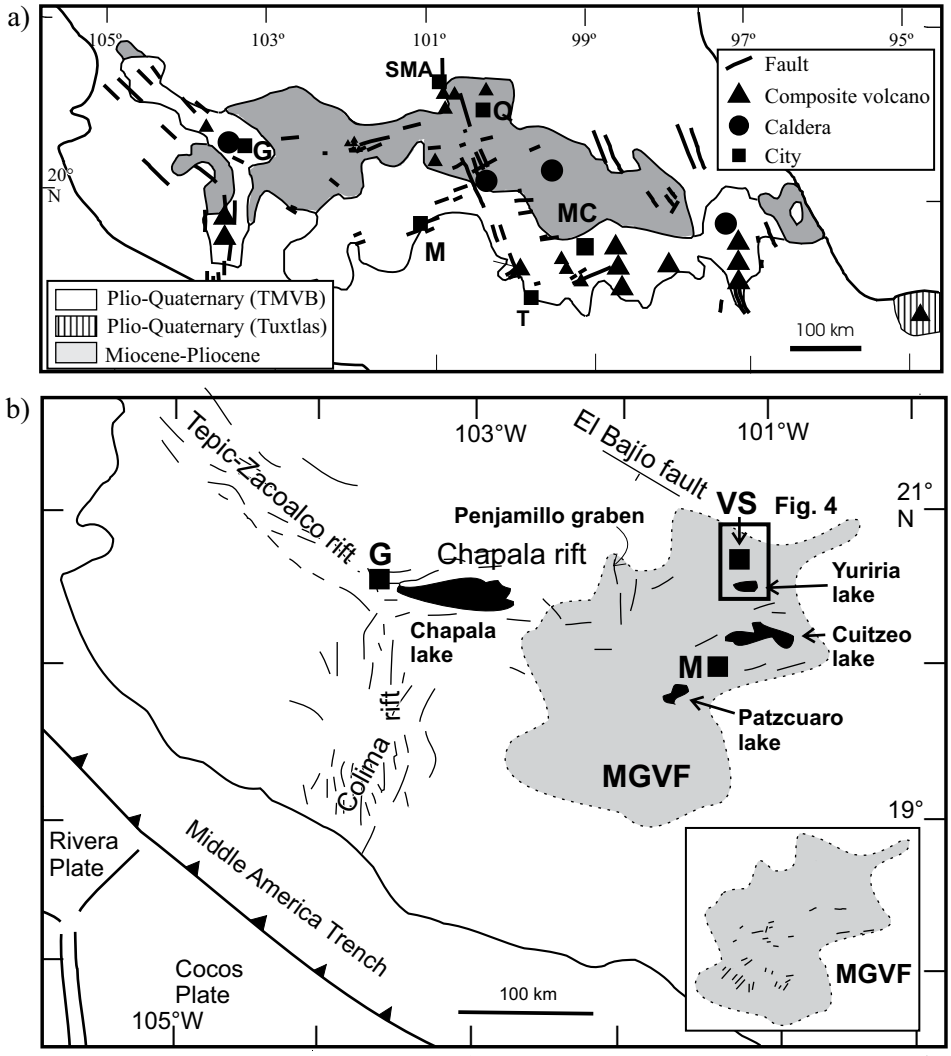

Figure 2. (a) The Plio-Quaternary volcanoes of the TMVB are located near the Middle America trench. Close to Guadalajara (G) there is a triple junction where three active rifts intersect. (b) The MGVF is located in the central part of the TMVB, west of the Taxco (T) – San Miguel Allende (SMA) fault system. Near the northwestern end of the MGVF are the N-S-trending Penajamillo graben and the N50W-trending El Bajío fault. Inset in figure (b) shows the volcanic lineaments identified by Connor (1990) in the MGVF. Note that these volcanic lineaments are roughly parallel to the convergence vector near the trench and parallel to the Chapala rift farther north. Other localities in the figures are: MC = México City, M = Morelia, Q = Querétaro, and VS = Valle de Santiago (Aranda-Gómez *et al.*, 2013).

lite-bearing lavas (*e.g.* Righter and Carmichael, 1993; Ortega-Gutiérrez *et al.* 2014), which are characteristic of some of the intra-plate magmas in the Mexican Extensional Province (Aranda-Gómez *et al.*, 2007)

The volcanic front (*i.e.* the loci of recent or active volcanism) of the western and central parts of the TMVB is located along an imaginary line that joins the historically active volcanoes: Colima, Paricutin, Jorullo, and Popocatepetl (Figure 2a). Quaternary cinder cones and maars as young as 0.07 Ma (K-Ar: Murphy, 1986) of the Valle de Santiago region are located 100 km north of the volcanic front as a consequence of the subduction of the Orozco Fracture Zone, which causes a pronounced indentation in the volcanic front known as the Tzitzio gap (Figure 3: Blatter and Hammersley, 2010). In addition to young cinder cones and maars, in the region around Valle de Santiago occur mid-size continental calc-alkaline lava shields, which are older (K-Ar: 2.1 to 6.8 Ma; Murphy, 1986; Ban *et al.*, 1992) and commonly have chemical compositions that are different from that of the mildly alkaline to alkaline cinder cones and maars (Murphy, 1986). Some of the Valle de Santiago maars were excavated in these older lava shields and, as we will see at the walls of La Alberca and Rincón de Parangueo maars, the andesitic lava flows of the older shield volcanoes are clearly exposed on the walls of the maar craters.

Volcanic features dominate the outcrop geology of the region around the town of Valle de Santiago. In the area covered by the map in Figure 4 we have recognized at least 50 cinder cones, 23 maar-type volcanoes and 14 lava shields. North and east of the town is a broad plain covered by alluvium, which probably represents the bottom of an extensive paleolake. The Yuriria Lake, located 15 km south of Valle de Santiago, probably represents the remnant of that paleolake. The phreatomagmatic volcanoes define a rough N25W-trending, 55 km long alignment of volcanoes, which extends from the shores of the Yuriria Lake to the outskirts of the city of Irapuato (Aranda-Gómez *et al.*, 2014b). Cinder cones around Valle de Santiago define lineaments with two different orientations (N55W and N80E) and the lava shields apparently are randomly distributed in the area covered by Figure 4, but they appear to be aligned in a rough ENE direction, as seen in Figure 1. Hasenaka and Carmichael (1985) reported a total of 20 maar type volcanoes in the MGVF; most of them are in the Valle de Santiago area. These facts argue about special hydrological and volcano-tectonic conditions in the region, as compared with the rest of the MGVF, where both maars and volcanic lineaments are generally scarce, and those vent alignments recognized are parallel to the direction of the plate convergence (N20-40E: see inset in 2b) as documented at the southern end of the MGVF (Connor, 1990).

Regional tectonic setting

The area between Querétaro and Valle de Santiago is located at the intersection of three regional fault systems (Figure 2b): Taxco – San Miguel de Allende (N20W), Chapala rift (N70E) and El Bajío (N50W). All these structures have had Neogene or Quaternary activity and together with the volcanic edifices control the landscape in the region.

The Chapala rift (or Chapala-Tula fault system: Johnson and Harrison, 1990) trends approximately ENE-WSW in the northern part of the MGVF (Figure 1), but the rift morphology it is not as evident as in the other two rifts in the western portion of the TMVB: the Colima and the Tepic-Zacoalco rifts (Hasenaka

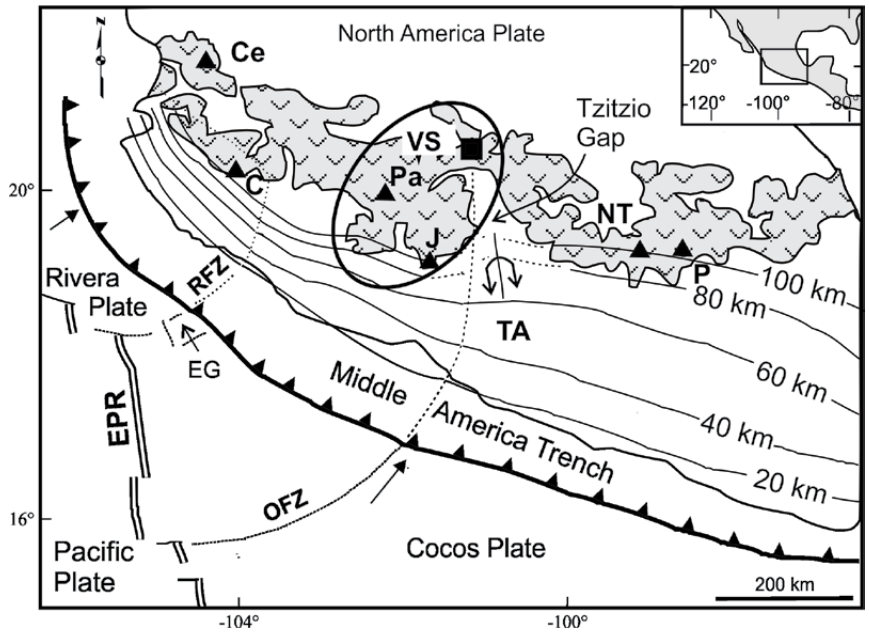

Figure 3. Quaternary volcanism in the TMVB is shown with ^ pattern. Inset box shows the area covered by the figure. The tectonic features on the ocean floor are modified from Pardo and Suárez (1995) and abbreviations used are: EG=El Gordo Graben, EPR=East Pacific Rise, RFZ=Rivera Fracture Zone, and OFZ=Orozco Fracture Zone. The depth to the subducting slab in km is shown with solid black contours (from Pardo and Suárez, 1995). Abbreviations: MGVF=Michoacán-Guanajuato Volcanic Field, VS=Valle de Santiago, TA=Tzitzio Anticline. Volcanoes located in the active volcanic front are: C=Fuego de Colima, Ce=Ceboruco, J=Jorullo, Pa=Paricutín, and NT=Nevado de Toluca. Simplified from Blatter and Hammersley (2010).

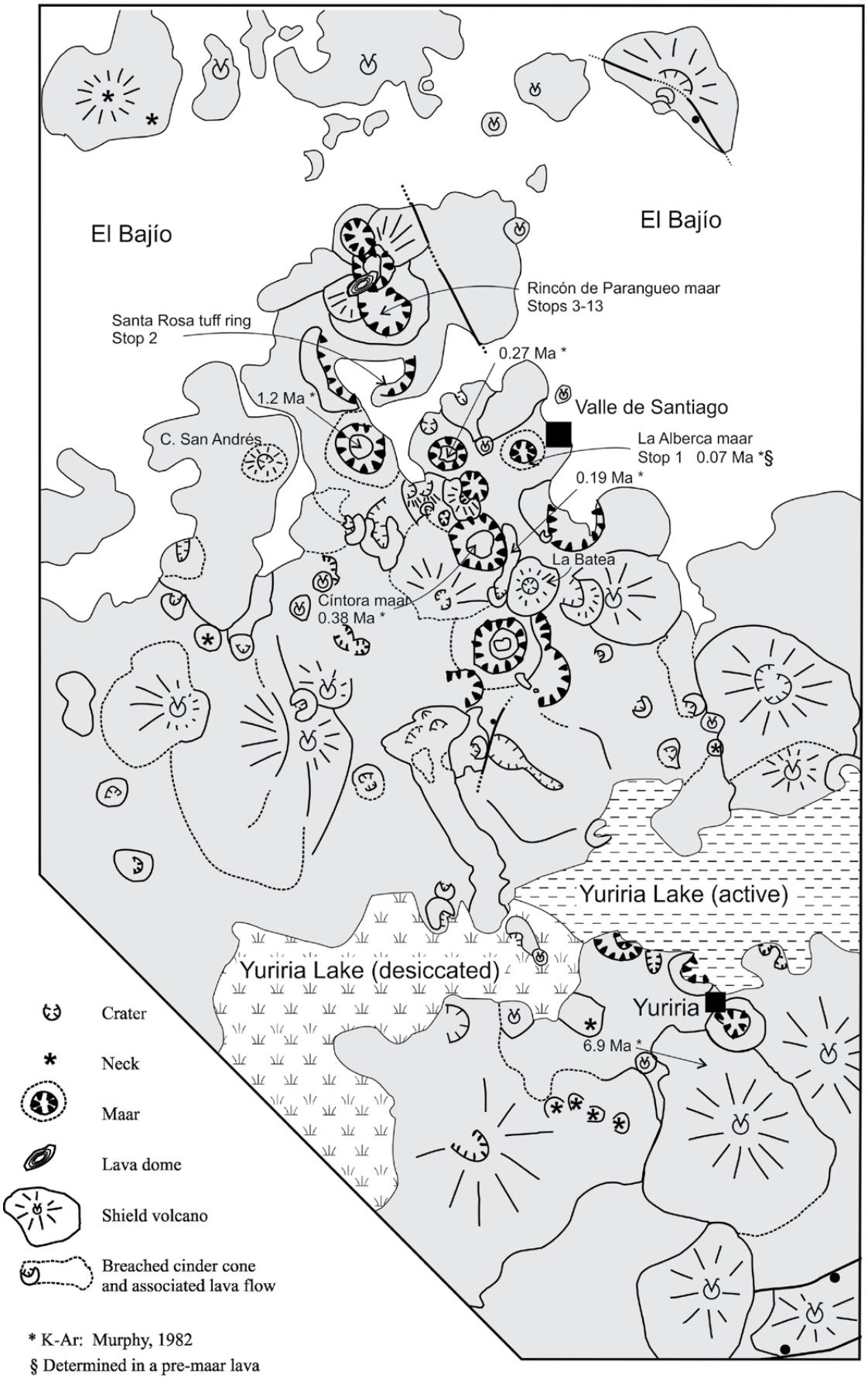

Figure 4. Photogeologic map of the Valle de Santiago region (Aranda-Gómez *et al.*, 2013).

1992a). The lakes Pátzcuaro, Chapala, Cuitzeo, and Yuriria occupy tectonic depressions at the Chapala rift (Figure 2b). Some of the medium sized volcanoes of the MGVF are cut and offset by the normal faults of the Chapala rift (Hasenaka, 1992b) and the rough alignment of shield volcanoes and the N80E cinder cone alignments around Valle de Santiago appear to be related to it. In addition to the ENE-WSW trend of normal faults, in the northern portion of the MGVF there is at least one N-S trending normal fault array known as the Penjamillo graben (Figures 1 and 2b). Shield volcanoes appear to be absent near this structure (Hasenaka, 1992b). This graben was studied by Martínez-Reyes and Nieto (1992) and it may still be active (Johnson and Harrison, 1990).

The MGVF appears to end on its northeastern part at the Taxco – San Miguel Allende fault system. This system is a ~N20W-trending array of normal faults that crosses the TMVB (Alaniz-Álvarez and Nieto-Samaniego, 2002), cutting some of the volcanoes and in some places is buried by volcanic and volcaniclastic rocks. There is geophysical evidence that the Taxco-San Miguel Allende is a major crustal discontinuity (Molina-Garza and Urrutia-Fucugauchi, 1994; Urrutia-Fucugauchi *et al.*, 1995; Arzate *et al.*, 1999). On the surface, the Taxco – San Miguel Allende system separates two segments in the TMVB with contrasting morphologies and styles of volcanism. Caldera and lava dome complexes of intermediate to felsic composition and associated ignimbrites are common east of the fault system in an area with abrupt topography. West of the fault system, on the down thrown side of the fault system is the MGVF and the broad El Bajío plain, which is locally interrupted by shield volcanoes and cinder cone and maar complexes.

Land subsidence and groundwater drawdown

Land subsidence is the lowering of the land-surface elevation caused by underground changes. Land subsidence is commonly related with excessive groundwater pumping, and/or intense oil and/or gas extraction. Subsidence is also linked to limestone or evaporite solution by groundwater and to collapse of underground mines, hydrocompaction (initial wetting of dry soils), and drainage of organic soils (Leake, 2010).

Aquifer systems that are susceptible to trigger land subsidence are those that have next or within them clay or silt beds. Lowered water pressure in sand or gravel beds lowers the water pressure and causes slow drainage of water from the inter-bedded clay and silt beds. Because these beds are compressible, they compact, causing land subsidence in the surface. Differential compaction within the system causes the formation of fractures, which often propagate to the surface. Relative displacement of blocks separated by the fractures act as "aseismic" faults, with displacement rates in the order of a few millimeters to centimeters per year.

El Bajío plain is characterized by intensive agriculture. Water for irrigation comes from the Ignacio Allende reservoir, located near San Miguel Allende (Figure 1) or from water wells. The Valle de Santiago – Salamanca aquifer has an estimated area of 1700 km^2 and provides water for 800,000 people. The number of active wells in 2008 was 1600 and the estimated volume of water extracted was 646×10^6 m^3/year. Drawdown rate in the past 25 years was estimated at 2 m/year. The extracted water was used as follows: agriculture 81%, urban supply 10%, industry 8%, and cattle raising 1% (Hernandez, 2007). As pointed before, soil fracturing and formation of active aseismic faults is one of the consequences of land subsidence. This phenomenon is common and widespread in the regions with a high density of wells, where intense groundwater pumping has formed cones of depression. Land subsidence-related active fractures have been documented in many urban areas of El Bajío, such as Querétaro (Pacheco-Martinez, 2007), Celaya, Salamanca, Abasolo, Silao, and Irapuato (Figure 1). A 12 km long, NE-trending, subsidence-related, active fracture occurs 16 km north of the center of the Rincón de Parangueo maar (Figure 4), near the oil refinery of Salamanca (Borja-Ortíz and Rodríguez, 2004). The estimated displacement rate in this man-induced normal fault is about 6 cm/year.

Active land subsidence and formation of landslides inside Rincón de Parangueo

One of the most striking topographic features at the bottom of the Rincón de Parangueo maar is a steep scarp located between the center of the dry lake and the former lake shore. This landform, unique among the phreatomagmatic craters of the Valle de Santiago region (Figure 5), is probably related to land subsidence caused by lowering of groundwater table during the last 3 or 4 decades (Figure 6). Air photos taken in March 1984, close to the end of the dry season, show a nearly circular lake with a diameter of 1100 m. Escolero and Alcocer reported that in 2003, just before the beginning of the rainy season, the lake was completely dry. The air photo shown in Figure 6c, shows a substantial area at the bottom of the crater covered with water. Presumably that water was accumulated during the wet season (May – September) of that year. Once the desiccation was completed, around 2003, the crater started to act as a playa-lake, which gathers rainwater during the wet season, and shrinks or completely dries during the dry season. Thus, the crater no longer acts as a discharge area for the regional aquifer, but it may act as a local recharge area with some unusual consequences related to the fact that water in the original crater-lake was highly alkaline.

A close inspection of the topographic scarp in the former lake bottom suggests that active deformation is occurring in the maar. We interpret the scarp as the trace of an active, segmented, ring fault. Cumulative

Figure 5. Panoramic view of the bottom of Hoya Cíntora (one of the four maars that had perennial lakes in 1900), as seen from 20° 21' 04.15"N, 101° 12' 21.14"W in October of 2010 (see Figure 4 for location). Note that the bottom of the crater is a gently curved, concave upward surface with no structural evidences of land subsidence. Poorly developed microbialites occur near the former lake shore, which is marked by the vegetation line (Aranda-Gómez *et al.*, 2013).

normal displacement in the ring fault is accomplished through a series of several concentric, high angle, step faults. In several places of the scarp had occurred rotational landslides (Highland, 2004), and in other areas these slope processes still are acting. Thus, structures such as dilational crown fractures, transverse cracks and ridges, rotated blocks, antiforms, synforms, and areas of complex deformation may be observed in different places near the scarp. The area located between the former perennial lake shore. and the edge of ring fault scarp probably was a gently inclined surface, tilted 2 – 3° towards the basin's depocenter. On this area grew a biostrome made of stromatolites, which we view as a slightly lithified, resistant (as compared with the calcareous mudstone accumulated in deeper water) carbonate platform (Figure 7). Near the edge of present day topographic scarp, stromatolites grew as a chain of bioherms, up to 1 m higher than the surrounding biostrome (Aranda-Gómez *et al.*, 2014c). It is worth stressing that bioherms and the outer part of the ring-fault zone coincide throughout the basin, a fact that may be related to the buried diatreme – country rock contact, as we will discuss in Stop 13 of this field trip.

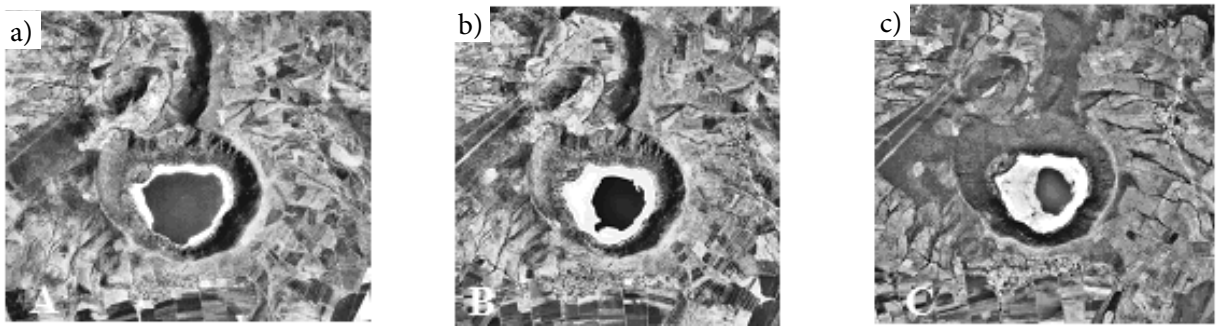

Figure 6. Vertical air photos of the Rincón de Parangueo maar taken in three different dates. Both (a) and (b) were taken close to the end of the dry season; they show that the lake inside the crater was shrinking. Escolero-Fuentes and Alcocer-Durand (2004) reported that by the end of 2003 dry season the crater was completely dry. Thus, the water shown in (c) was accumulated from rain from the end of May to September of 2003. Size of the lake during our visit in the 5IMC is likely to be similar to that shown in (c), Aranda-Gómez *et al.*, 2013.

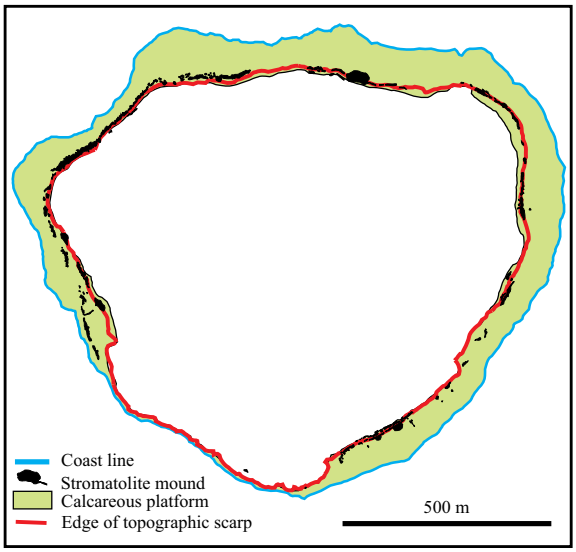

Figure 7. The carbonate platform near the former lake shore of Rincón de Parangueo. Stromatolite bioherms occur throughout the platform, close the fault scarp (Aranda-Gómez *et al.*, 2014c).

Precipitation of trona

The presence in the lake sediments of trona [$Na_3(CO_3)(HCO_3)$ * $2(H_2O)$] and other sodium carbonates such as thermonatrite [Na_2CO_3 *H_2O], natrite [Na_2CO_3], and eitelite [$Na_2Mg(CO_3)_2$], together with halite [NaCl] and sylvite [KCl]indicate evaporate precipitation from Na^+ – HCO_3-type water produced by silicate hydrolysis of volcanic rock or volcaniclastic sediments. However, it has been noticed that not all the hydrological basins that meet these general requirements produce significant amounts Na–CO_3 minerals. An additional factor for trona precipitation is a high partial pressure of CO_2. Earman *et al.* (2005) proposed that an input of magmatic CO_2 can influence water chemistry in such a way that trona would precipitate upon evaporation. In the case of Rincón de Parangueo we believe that an alternative source of "excess" CO_2 in a system could be related to organic decay or microbial action. We have noticed that evaporitte precipitation begins as soon as the wet season ends and reaches a maximum at the end of the dry season, when the remnant water in the playa-lake becomes dark red, as a consequence of bacterial and/or algal blooms. This issue about the origin of excess CO_2 remains to be investigated.

Discussion

We consider maar desiccation in the Valle de Santiago area as a consequence of drawdown in the Valle de Santiago – Salamanca aquifer (Aranda-Gómez *et al.*, 2009, 2013). Therefore, subsidence of the bottom of the crater could be in part, associated to this phenomenon as significant compaction of the fine-grained lake sediments is probably occurring. A comparison between the mean subsidence velocity in the Salamanca fault (6 cm/year) and the much higher subsidence rate indicated by the collapse structure inside the crater (≥50 cm/year; assuming that the ≥10 m high topographic scarp was formed in the past 20 years or >40 cm/year if it was formed in the past 35 years) suggests that an additional process may be operating inside the crater. Presence of a significant amount of the water-soluble salts, such as halite, sylvite, trona, and other Na carbonates was established by us using XRD in a mud sample collected near the remnants of the playa-lake. In a simple test to estimate the amount of soluble minerals in a small lake sediment sample, collected near the shore of the present day playa-lake, ~33 wt% of the previously dried sample was easily dissolved in distilled water at room temperature. Thus, the remarkable collapse features observed at the bottom of the crater may have been in part formed in a similar way to the sinkholes studied by Closson (2004, 2005) around the Dead Sea. Closson (*op. cit*) first proposed a model where the flow of unsaturated groundwater dissolved concealed evaporite layers, which caused the formation underground cavities that later collapsed, producing sinkholes on the surface. In this context, it is worth mentioning that nowhere at the bottom of the crater has been observed a continuous, thick evaporite layer. Visible salts are only present around the remaining water at the end of the dry season, where they precipitate every year.

We view the Rincón de Parangueo maar as a partly closed system. Rainwater that falls inside the crater's closed basin feeds an ephemeral playa-lake in recent years. Rain freshwater can dissolve the soluble salts in the lake sediments and move them toward the playa-lake. We believe that each year at least a small portion of the newly formed brine infiltrates the ground and is incorporated into the regional aquifer, while the rest of the water is lost through evaporation, triggering the precipitation of water-soluble salts. We are trying to prove that underground water flow is now moving solutes into the regional aquifer. Residents of the area around the crater have noticed an increase in the salinity of the water in their wells in recent years. Our hydrogeochemical study of a large number of groundwater samples shows that the highest ion concentration, pH and water temperature occurs at Rincón de Parangueo, and steadily decreases away from the crater.

The structural attitude of the mudstone laminations in the blocks exposed in topographic scarp almost invariably dip toward the center of the crater and the area occupied by the scarp, as a whole, can be described as a monocline-like structure, modified by the presence of high angle normal faults, at least two conspicuous sets of extensional fractures and, in some places, by fractures caused by rotational slides. Dip angles in the mud laminations in the blocks exposed on the scarp vary from 10 – 15° near the outer edge of the scarp, to 25 – 45° in the middle part of the slope, to 10 – 15° near the base of the scarp. Thus, the struc-

ture, as seen on a vertical section perpendicular to the scarp, has the shape of a sigmoid curve. Departures of this basic shape are produced by the high angle normal faults and by rotational landslides growing on the topographic scarp. We interpret this overall structural disposition of the mudstone laminations as a forced extensional fold (Figure 8), similar to those developed above an upward propagating normal fault (Aranda-Gómez *et al.*, 2014a). However, in this case the "normal" component of the fault segments displacement are caused by differential subsidence, and the loci of the fault segments is the buried diatreme – country rock contact, which causes a large difference in the thickness of the highly compressible sediments and volcaniclastic rocks (i.e. the diatreme).

The steepening of the terrain as the bottom of the lake subsided probably triggered landslides observed around the collapse ring. This phenomenon probably started very early in the desiccation process, while the lake still had water and it is still acting. It is remarkable that the calcareous platform is completely missing in the southwestern portion of the lake's basin, an area where the sigmoidal curve disposition of the mud laminations appears to be absent in the nearly vertical scarp. In the same area landslide-related megabreccias and mud injection domes are abundant in the lower part of the basin. Despite the gentle slope of the dry lake bed in the area between the depocenter and the topographic scarp, down slope sliding of the mudstone is still occurring, as demonstrated by active faults that cut and displace some of the landslide related megabreccias (see Stop 8 description) and the largest mud dome in the crater (Figure 9)

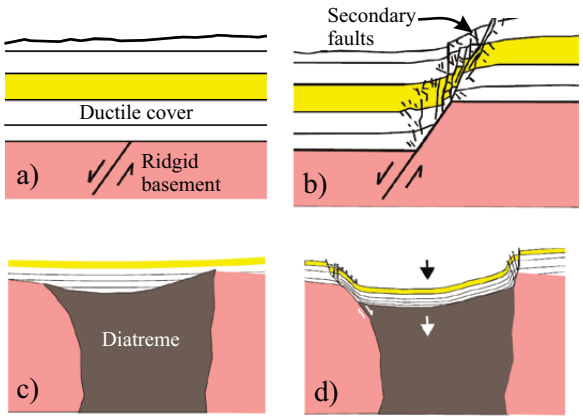

Figure 8. (a)-(b) Experimental clay model of extensional faultpropagation fold associated with an upward-propagating, normal fault involving a rigid basement and a ductile sedimentary cover (Whitjack *et al.*, 1990). (c)-(d) deformation at RP lake sediments occurred above the buried contact diatreme-country rock. "Normal movement" in the system is mimicked by differential compaction of the wet lake sediments at the bottom of the maar (Aranda-Gómez *et al*., 2014a)

ACKNOWLEDGMENTS

Financial support for our work in Valle de Santiago has been provided by grants Papiit IN109410-3 and Conacyt 129550, both to J. Aranda, and Conacyt grant 150900 to G. Carrasco.

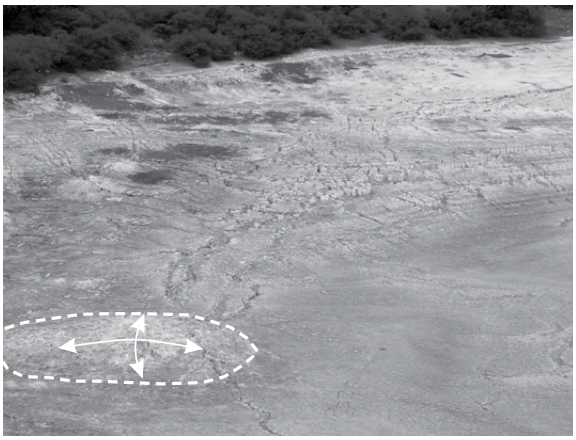

Figure 9. Active fault cutting the largest mud dome in the SW part of the lake bed.

§

PART II: STOP DESCRIPTIONS

Stop 1:
La Alberca: an overview of the interior of a young(<0.25 Ma) maar volcano and evidence of its recent desiccation. Discussion about magma-water fluctuation during the formation of a basaltic maar.

Hoya La Alberca is a quasi-circular-shaped crater 700 m in diameter. It is at the eastern end of an E-W alignment of four maars that intersect with a dominant, NW-trending, regional alignment of maars (Figures 1 and 4). In general, volcanic lineaments are interpreted as evidence of a structural control on the location of volcanism (*e.g.* Nakamura, 1977); it is assumed that magma reaches the surface through extensional fractures or faults. Joints and faults in hard rock also produce hydraulically active domains where groundwater is available in fracture-controlled aquifers (Lorenz, 2003).

Hoya is a term related to the Spanish word "hoyo", which means hole or pit. The word "alberca" signifies pool. This maar name is derived from the fact that for many years the crater-lake was used as a swimming pool by the locals (there is the framework of an abandoned springboard on the SW wall of the crater). Prior to the 1980's the lake at the bottom of the crater was permanent as it was fed by the Valle de Santiago– Salamanca aquifer (Figure 10a).Today, there is no longer a permanent lake inside the crater as a consequence of overdraft in the aquifer (Figure 10b, 10c). Groundwater in the region is mainly used for irrigation and to provide drinking water for a growing population in the region around Valle de Santiago and Salamanca. The maximum level the lake attained in the recent past is clearly marked by white stromatolites attached on the walls of the crater (Figure 10b). Based on the height difference between the white mark on the wall and the bottom of the dry lake bed and the date when the crater was desiccated Escolero-Fuentes and Alcocer-Durand (2004) estimated a drawdown rate for the Valle de Santiago – Salamanca aquifer of 2.6 m/year.

From the parking lot, located inside the crater (20° 23' 10.06"N, 101° 12' 06.65"W), looking towards the north, we will see the volcanic sequence exposed on the walls of the crater. Refer to panoramic views depicted in Figure 10.

The local geology of Hoya La Alberca is exposed on the crater walls (Figure 10c). Pre-maar rocks are andesitic lava flows with conspicuous vertical joints. These lavas are not related to the formation of La Alberca crater. The andesitic pre-maar lavas were dated by the Ar/Ar method at 0.25 +/- 0.02 Ma (Rincón, 2005). These lavas are separated from the maar-forming pyroclastic succession by a paleosol exposed at the base of the wall located immediately south of the parking lot (20°23'10.38"N, 101°12'8.25"W). This paleosol represents a significant period of repose between the pre-maar andesite and the formation of the maar. Thus, field relations and the Ar/Ar date indicate that the maar is younger than 0.25 Ma.

Prior to the formation of the maar, a small scoria cone was constructed at the area now occupied by the crater. Remnants of the cone are exposed at the NE wall of the crater (Figure 10b and 10c). It is likely that the summit area, crater and feeding conduit of the cinder cone were located towards the center of today's maar crater (Figure 11). The scoria cone indicates strombolian activity, characteristic of "dry" magmatic eruption prior to water-magma interaction. The scoria cone was formed by relatively short-lived eruptive columns that produced scoria and ash that accumulated close to the vent. The lack of a paleosol between the scoria-fall deposit and the phreatomagmatic succession, as it can be seen in the vertical wall exposed at 20° 23' 10.30"N, 101° 12' 08.21"W suggests that this activity was the precursor eruptive signal, which occurred just before the initiation of the more violent, maar-forming, phreatomagmatic explosions.

The pyroclastic succession produced by the maar-forming eruption is well exposed on the cuts of the access road. The succession was divided into 5 different members (Figure 12: intervals A thru E). The phreatomagmatic eruption started with very violent explosive activity caused mainly by phreatic eruptions although in some cases, when magma interacted with water, phreatomagmatic eruptions also occurred. This activity produced a very efficient fragmentation of the country rock and the magma forming a sequence dominated by fine-grained, laminar, surge beds deposited by pyroclastic density currents (A interval in Figure 12). Higher up in the stratigraphic succession, the fine-grained beds alternate with massive heterolithologic breccia, coarse gravel, and unsorted layers with some blocks within a sandy-silty matrix (B interval in Figure 12).

Some of the surge layers include thin horizons with accretionary lapilli, suggesting wet conditions during the transport of particles in surges (Brown and Branney, 2010). Most of the material involved in these deposits is accidental and came from andesitic lavas similar to those exposed near the base of the crater walls. Fragments of basaltic andesite, basalt, and altered volcanic rocks are also included, but usually in minor proportions. Juvenile clasts are highly vesicular, fresh-looking, megacryst-bearing, black scoria clasts. The proportions of juvenile material is variable through the succession; the highest juvenile fragment content (about 25 – 35 %) is found in just a few localized layers exposed at the base of the medial zone and at the upper sequence (E interval in Figure12).

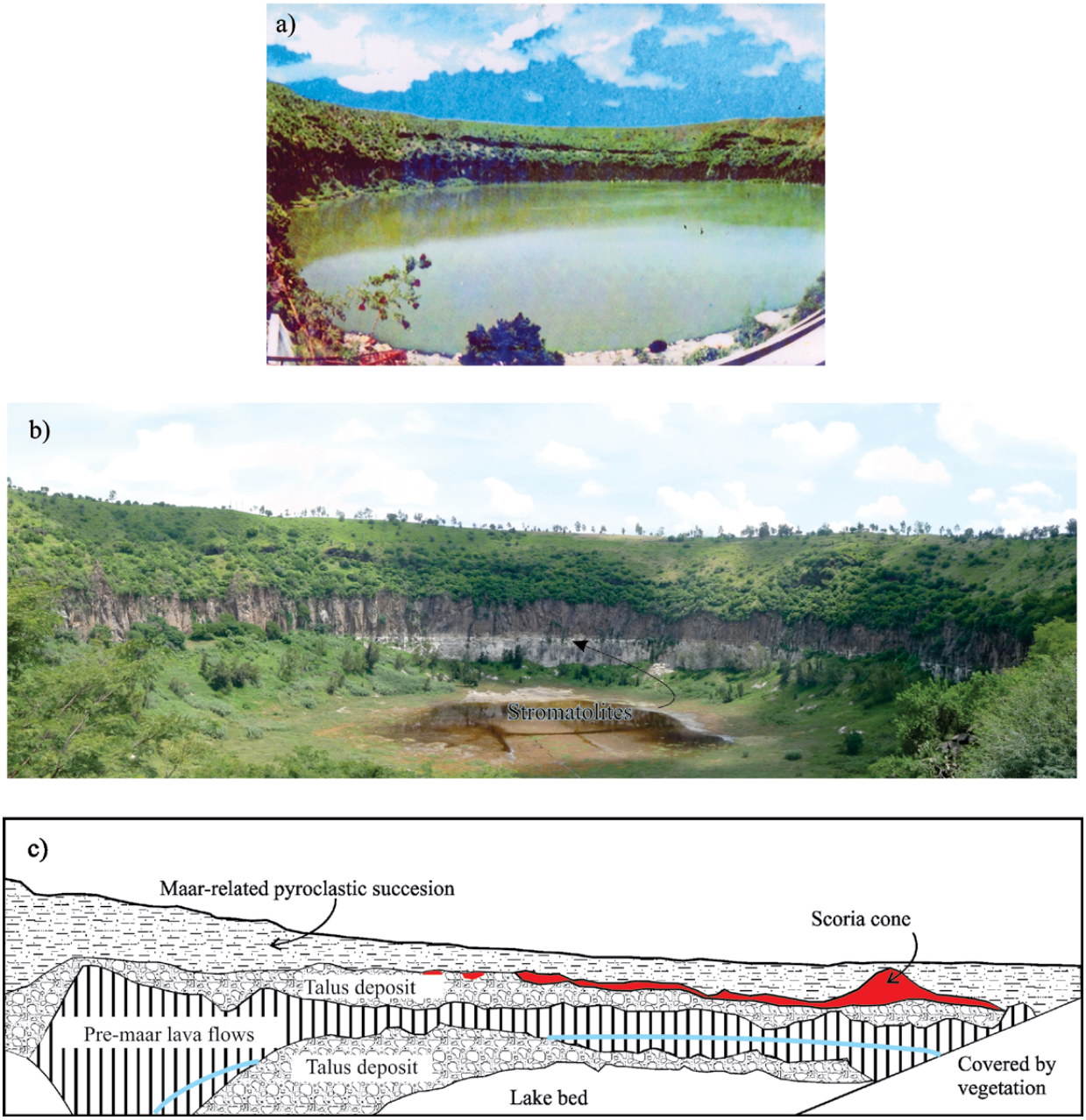

Figure 10. Panoramic views of La Alberca crater. (a) The northern wall prior to desiccation process (date when photograph was taken is unknown, but probably before 1985. This photograph is sold as a postcard in Valle de Santiago). (b) Approximately the same view, as seen in August 2010. Note that the small "playa-lake" has a slight red color, probably due to the presence of a cyanobacteria bloom in the water. (c) Line drawing enhancing the main geologic features shown in (b). (Aranda-Gómez *et al.*, 2013).

The basal scoria layer (Figure 12), located immediately above the paleosol, is interpreted as the product of strombolian precursor activity, which formed the scoria cone exposed on the northern wall of the crater and preceded the initial phase of the maar formation (Figure 12d).

In the medial part of the sequence (C interval in Figure 12), there is a marked increase of massive deposits with coarser granulometry, larger ballistic blocks, and thicker layers. This reveals a change in the water-magma interactions with less efficient fragmentation and less energetic eruptions. However, clear evidence of wet conditions is recorded in the deposit. This stratified succession includes layers with impact sags that resulted from ballistic blocks landing on wet sediments and producing ductile deformation in them. Asymmetry of in the folds underlying the ballistic clasts may be used to infer transport direction and approximate location of the vent which expelled the ballistics.

The upper part of the succession (D and E intervals in Figure 12) is dominated by massive breccia layers

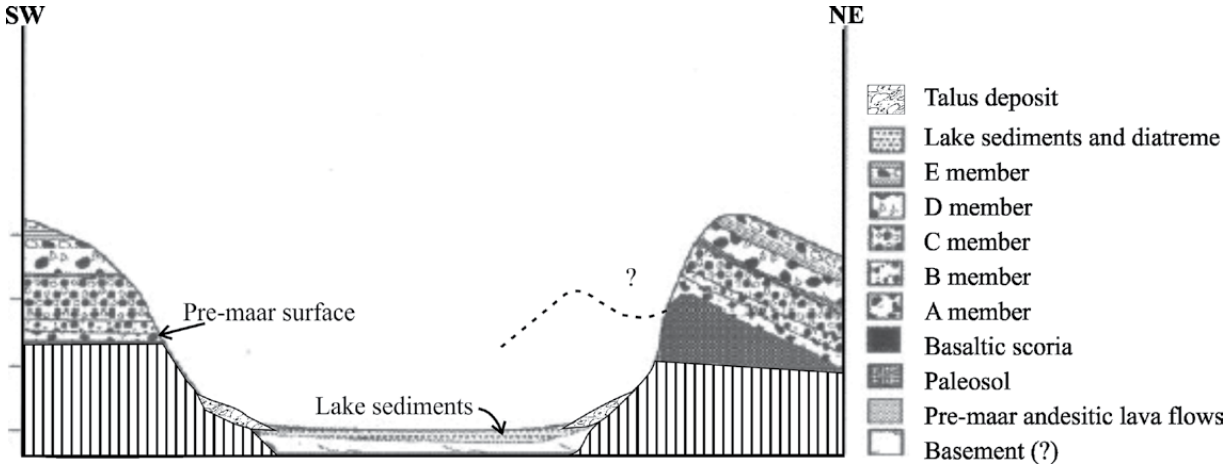

Figure 11. Schematic NE-SW cross section thru La Alberca maar. Note the hypothetical location of the vent of the scoria cone exposed on the NE wall (modified from Rincón, 2005).

with thinner sandy-rich layers. The breccia deposits in D show the largest blocks (up to 1.8 m in diameter) in the pyroclastic deposit. This succession changes upward to a thinly stratified alternation of gravel and sand-dominated horizons (E interval in Figure 12), some of them include well-sorted vesicular juvenile particles of basaltic composition that suggest that the aquifer was gradually drying out in the vicinity of the volcanic vent. However, the uppermost part of the sequence includes surge-dominated layers showing characteristic cross-stratification. Probably the final activity during eruption consisted of short periods of strombolian activity alternating with phreatomagmatic explosions.

The overall nature of the pyroclastic deposit (i.e. the different clast proportions and structures in the succession) indicates wide variations in the water-magma ratio in the system, which produced marked changes in the efficiency of fragmentation of both, juvenile and accidental components. Water-magma variations may reflect variable rates of magma injection and/or transient changes in aquifer in the immediate vicinity of the vent (formation of a cone of depression and/or temporary exhaustion of water). Changes in the water-magma ratio produced variable and rapid changes in the explosivity during the eruption. Molten-fuel coolant interactions (Zimanowsky *et al.*, 1997) were active during the second part of the eruptive process that originated this volcano

From the parking lot, 20° 23' 10.06"N, 101° 12' 06.65"W, looking towards the north, we will see the stromatolites that mark the highest water stand in the crater. Refer to panoramic views depicted in Figure 10.These microbialites, which commonly thrive in extreme conditions, give us hint about water composition in the desiccated crater-lakes of Valle de Santiago.

Ezequiel Ordóñez made the first geologic study of the volcanoes around Valle de Santiago in 1900 and clearly recognized their phreatomagmatic origin. Four crater-lakes existed in the area: La Alberca, Hoya San Nicolás, Hoya Cíntora and Hoya Rincón de Parangueo (Figure 13) prior to the intensive overdraft in the Valle de Santiago – Salamanca aquifer (Figures 5, 6 and 10). Today there are only small pools of water in all of them during and after the rainy season. Water composition (Table 1) of the lakes prior to the desiccation process is only known for La Alberca (Escolero-Fuentes and Alcocer-Durand, 2004). However, La Alberca crater-lake, according to the local people, was considerably less saline that Rincón de Parangueo. Presumably water at Hoya San Nicolás and Hoya Cíntora had even lower concentrations of salts than La Alberca and Rincón de Parangueo. It is worth noting that stromatolites commonly are extremophiles and that they are considerably better developed at Rincón de Parangueo, where today´s water pH is > 10 and water's salinity is larger than in any of the other craters (Table 2). Thin, dusty, coating of salts that occasionally can be seen covering the lake sediments in isolated patches evidences presence of a relatively high salinity in San Nicolás and La Alberca's playa-lakes water. In addition to this, we note that the best developed stromatolites occur at the calcareous platform of Rincón de Parangueo, followed by the stromatolites that grew attached to La Alberca's pre-maar lavas, whereas thin ($\leq$ 2 mm) carbonate crusts occur only in some of the rocks located near the lake shores of Cíntora and San Nicolás. Thus, it seems that vigorous growth of microbialites was related with high salinities in the water of the original crater-lakes.

The topography of the bottom of the perennial lake that formerly occupied the San Nicolás crater is a smooth, gently curved, concave upward surface, without any evidence of post-desiccation sinking. A similar topography is observed both at La Alberca and Hoya Cíntora, between the talus deposits at the base of the pre-maar lava flows and the depocenters (Figures 5 and 10).

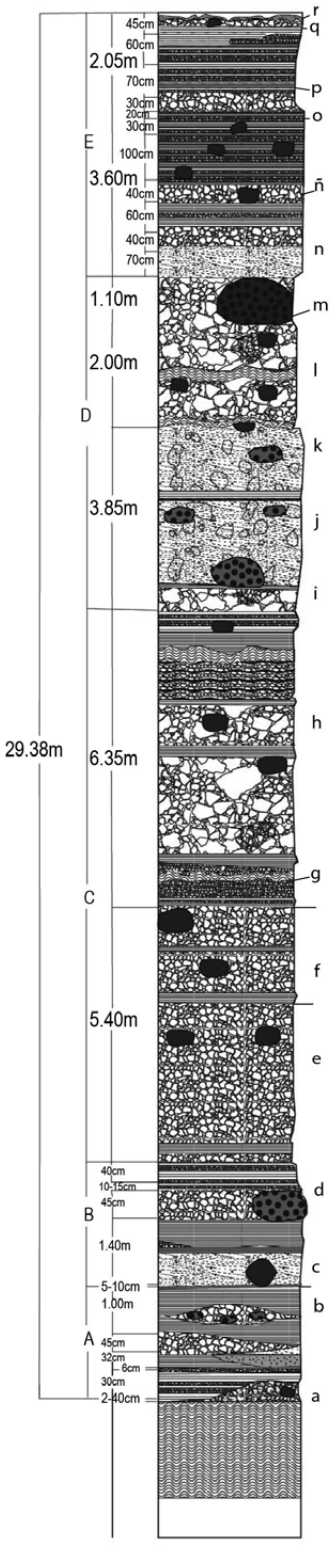

Sequence of thinly stratified gravel and sand-dominated layers with a few horizons including basaltic juvenile clasts in the middle part. Surge layers with cross stratification are shown at the topmost horizons

Sequence of massive breccia-dominated layers including the largest blocks (up to 1.8 m), with thin fine-grain layers.

Thin stratified sequence of massive breccia-dominated layers with minor stratified sandy-silty layers, with laminations showing cross stratification and impact bombs at the upper part.

Alternated sequence of massive breccia with stratified sandy-silty layers with sedimentary structures.

Surge (fine-grain)-dominated layers with minor stratified gravels: accrecional lapilli in some layers.

Basal scoria layer

Paleosoil

Pre-maar andesitic lava flows

Figure 12. Stratigraphy of La Alberca's pyroclastic succession, exposed along the access road to the crater. Based on lithologic variations, the succession was divided into five stratigraphic intervals (A thru E).

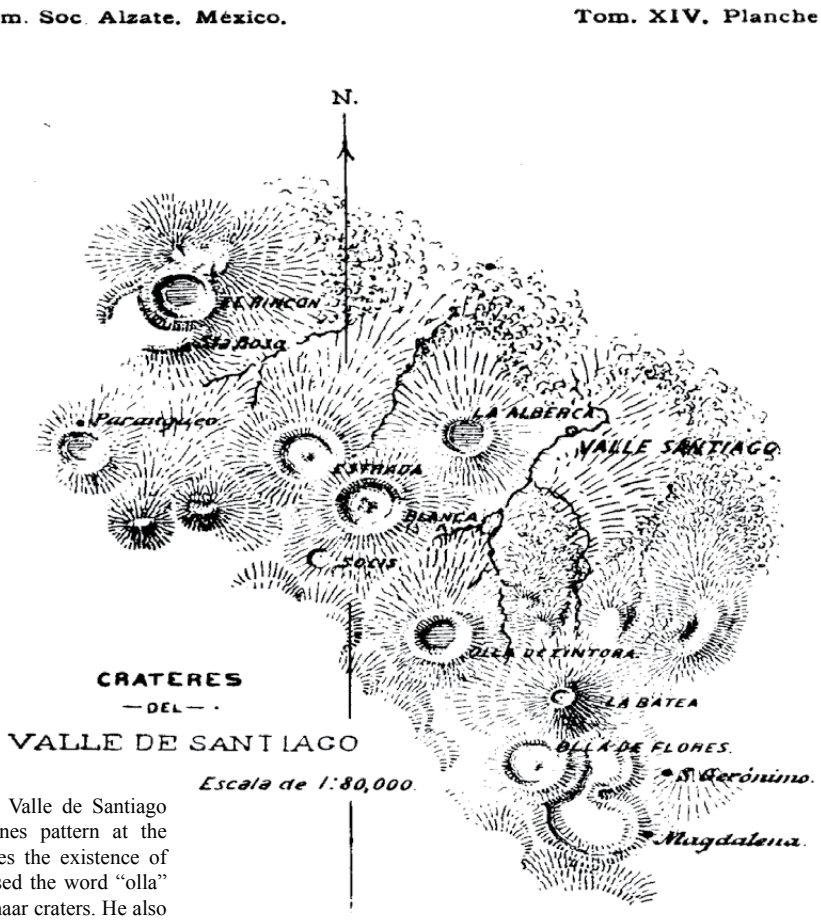

Figure 13. Ordoñez's 1900 map of the Valle de Santiago volcanoes. Note that the horizontal lines pattern at the bottom of crater-lakes, which symbolizes the existence of lakes. In this particular map Ordóñez used the word "olla" (pot) instead of "hoya" for some of the maar craters. He also spelled Cíntora as Zíntora.

Stop 2

An overview of the Parangueo volcanic complex as seen from the southern rim of the Santa Rosa de Parangueo tuff ring.

We will see the cross cutting relations between several volcanoes from a vantage point located 20°24'36.09"N, 101° 15' 8.34"W near the pyroclastic sequence of the Santa Rosa tuff ring. Refer to Figure 4 for location of the stop and to the geologic map of the complex (Figure 14).

The Parangueo volcanic complex is formed by at least six volcanoes. Three Quaternary phreatomagmatic volcanoes were excavated in an older (Pliocene?) trachyandesitic lava shield. Inside the crater of La Mina maar grew a rhyolitic lava dome; its silica-rich composition contrast with the intermediate or mafic composition of other volcanoes in the complex. The juvenile material of the Santa Rosa tuff ring, collected in a quarry near the church, located at 20°24'42.31"N, 101°14'35.04"W yielded an Ar/Ar age of 0.137 ± 0.09 Ma (Aranda-Gómez *et al.*, 2009).

Figure 15 shows a panoramic view of the complex as seen from the Santa Rosa de Parangueo church. The gentle outer slopes of the lava shield are obvious, as well as the Rincón de Parangueo maar crater and the rounded hill of the lava dome. The flat surface at the bottom of the tuff ring is a playa-lake during the wet season; it also represents the remnant of the larger regional paleolake. Figure 16 is an epipolar image, which allows, with the use of anaglyph glasses, seeing a 3D air view of the complex.

Table 1. Chemical composition of La Alberca water (modified after Escolero-Fuentes and Alcocer-Durand, 2004). The 1941 data is based on Orozco and Madinaveitia (1941), which reported the existence of a spring that fed the crater-lake. Location of the spring is unknown.

Ion	Spring	Craterlake	
mg/l	1941	1941	1981
Na	102.2	2933	448
K	n.d.	n.d.	88
Ca	Tr	Tr	6
Mg	Tr	Tr	70
SO_4	8	412	73
Cl	21	504	174
HCO_3	225	2127	811
CO_3	0	2094	204
NO_3	n.d.	n.d.	1

Tr = trace; n.d. = not determined.

Table 2. Field parameters and water chemistry of Rincón de Parangueo and La Alberca crater-lakes after the rainy season in 1999 (compiled from Armienta *et al*., 2008).

	Depth	T (°C)	pH	Λ (μS/cm)	Tot alk	Na^+	K^+	SO_4^{2-}	Cl^-	B	SiO_2	CO_3^{2-}	HCO_3^-	Date
Rincón	Surf	18.1	10.2	165,000	76,000	4,250	5,070	76	64,000	414	29	40,000	12,000	10-99
Rincón	5 m	23.6	10	n.d.	n.d.	n.d.	n.d.	n.d.	n.d.	n.d.	n.d.	n.d.	n.d.	10-99
Alberca	Surf	21.3	9.6	11,960	5,825	3,102	530	536	2,400	13	11.3	2,913	1,185	10-99
Alberca	4 m	19.3	9.7	12,460	n.d.	n.d.	n.d.	n.d.	n.d.	n.d.	n.d.	n.d.	n.d.	10-99

T = temperature, Λ = electric conductivity, Tot = Total alkalies, Surf = surface. All concentrations in parts per million.

Stop 3

Rincón de Parangueo maar. Further evidence of desiccation of the crater lakes of Valle de Santiago due to overdraft in the Valle de Santiago – Salamanca aquifer. Landslides triggered by land subsidence caused by sediment compaction and/or dissolution of evaporites. Stromatolites: living fossils that thrive in extreme environments.

Buses will park at 20° 25 ’18.22” N, 101° 14’ 51.39” W. From there we will walk 100m through the town to the entrance of a tunnel (20° 25’ 20.51”N, 101° 14’51.22” W) that leads to the interior of the crater. The tunnel is approximately 400 m long and is not illuminated. In several places the tunnel’s roof is low, about 1.7 m (5’ 8”) high. Please exercise extreme caution to avoid head injuries. Those of you that do not have a lantern, please join other attendees that carry lanterns. Coming out of the tunnel (20° 25’ 33.54”N,101° 14’ 53.07”W) we will find a small platform where we can stand and take a first look to the crater’s interior (Figures 17 and 18). The most prominent features seen from here are:

1. The lake sediments at the bottom of the crater have a striking white color. This feature is related to the mineralogical composition of the sediment, which is made of hydromagnesite [$Mg_4(CO_3)_4(OH)_2.4H_2O$]. Locally, near the playa-lake, there are abundant evaporites covering the sediments.
2. There is only a relatively small remnant of the lake east of the center of the basin. This water comes from the rain and may completely disappear close to the end of the dry season (April-May).
3. A conspicuous topographic scarp is located between the former shoreline, marked by the contact between the white sediments and the vegetation, and the depocenter. This topographic feature is continuous around the crater and it is interpreted as product of sediment down-sagging and normal faulting (Figure 20). The fault system is annular. Individual faults are segmented and almost invariably with the downthrown block towards the depocenter.
4. A nearly horizontal calcareous platform (Figure 7) is located between the former shoreline and the topographic scarp. This feature has variable width

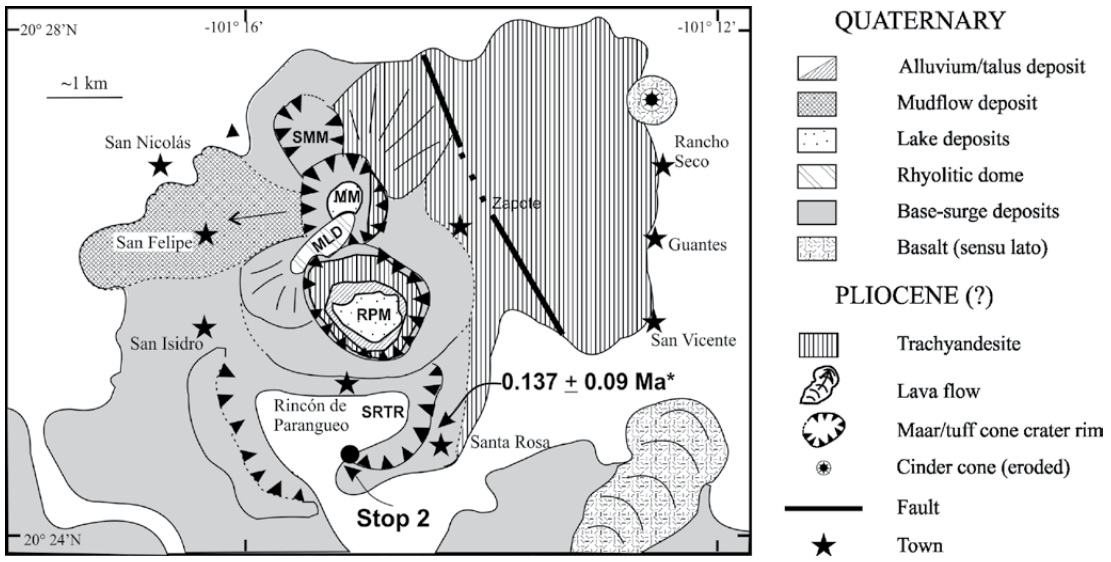

Figure 14. Geologic map of the Parangueo volcanic complex. Three maars were excavated in trachyandesitic continental lava shield. Remnants of a tuff ring are also exposed. Inside La Mina maar (MM) grew a rhyolitic lava dome (Figure 15). Key: SMM = San Manuel maar, MLD = La Mina lava dome, RPM = Rincón de Parangueo maar, and SRTR = Santa Rosa tuff ring (Aranda-Gómez *et al.*, 2013).

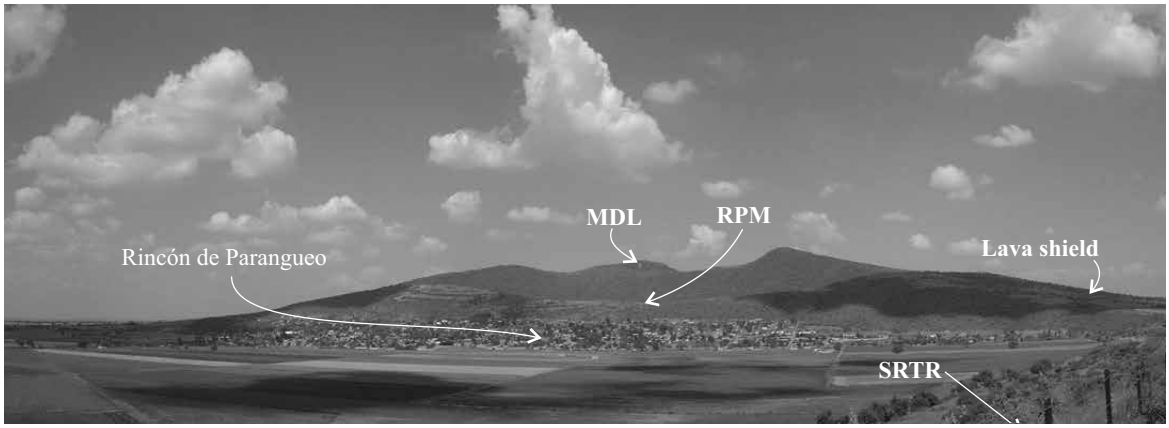

Figure 15. Panoramic view of the Parangueo volcanic complex, as seen from the south (Aranda-Gómez *et al.*, 2013).

and it is almost continuous around the lake basin. A remarkable exception is just below the place where we are standing. At that point, as we will see toward the end of the day, several landslides destroyed the platform.

5. Most of the pyroclastic sequence associated to the maar is covered by vegetation. However, some stratified rocks can barely be seen near the edge of the crater.
6. Subsidence related deformation is not uniform in the carbonate platform. We have identified several deformation domains in the topographic scarp and adjacent areas. The southern and eastern portions of the scarp are characterized by the presence of normal faults with listric planes and rollover anticlines. Near the base of the scarp mud domes and anticlines are conspicuously absent. Mud domes and folds are abundant near the base of the scarp in

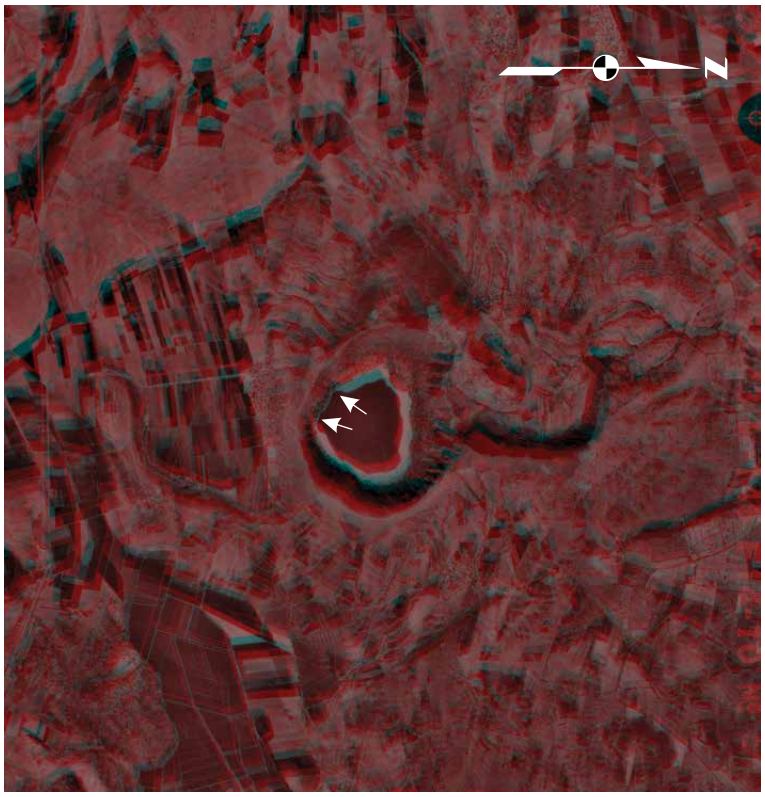

Figure 16. Epipolar image of the Parangueo volcanic complex obtained from a 1:75,000 air photo stereo pair taken in March 1984. The use of anaglyph glasses is required to see the 3D. Compare with geological map in Figure 14. The irregular-shaped white ring roughly corresponds to the calcareous platform (Figure 7) prior to formation of landslides. White arrows 1 and 2 shows landslide scarps formed prior to the total desiccation of the crater-lake. Thus, we believe that subsidence and mass wasting began before 1984, while the crater still had a considerable amount of water. Note NW-trending lineaments, SW and NE of the maars; they are interpreted as normal faults (Aranda-Gómez *et al.*, 2013).

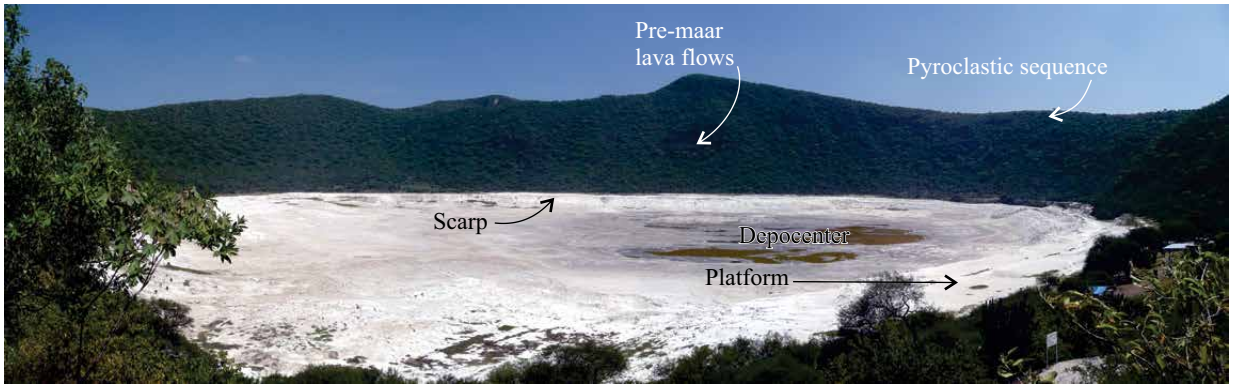

Figure 17. The bottom of the Rincón de Parangueo crater, as seen from the access tunnel exit.

the western and southwestern sectors of the scarp. The northern part of the calcareous platform is relatively well preserved and rollovers and domes are scarce or absent (Figure 18).

Stop 4

Rollover domain: incipient faulting in the southern part of the lake shore; in some places the stromatolite biostrome is tilted toward the shoreline as a consequence of normal faulting on a listric surface still hidden.

From the tunnel entrance we will follow a cobbled trail to a picnic area located on the southern part of the crater´s bottom (20°25'37.47"N,101° 14' 52.27"W).

In the area located between the park and the topographic scarp (Figure 19) is exposed a platform covered by a biostrome of stromatolites. These microbialites, made of aragonite, magnesian calcite and dolomite, form a blanket-like mass of poorly indurated rock. Just at the edge of the platform exists several stromatolite bioherms (mound-like colonies). The distinctive structure of the stromatolites is almost completely destroyed in the biostromal part of the ring at this locality as a consequence of heavy visitor traffic.

Throughout this part of the platform there are fractures and small displacement normal faults that mark the beginning of an incipient landslide. Some of the tensional fractures are clearly open and may have some vertical displacement. Other fractures are barely visible and lack displacement. As a general rule, cumulative vertical displacement in the fracture system gradually increases as one gets closer to Stop 5. Note that the stromatolite platform dips gently (4° SE) towards the lake shore as a consequence of block rotation associated to listric planes in the active normal faults.

At the edge of the main topographic scarp it is possible to see a 2 m displacement of the stromatolite bed. Total displacement in the ring fault system is accomplished several parallel, nearly vertical, step faults. A feature that can be seen on the fault scarp is that underneath the stromatolites there is a one meter thick tufa bed composed by Ca, $Mg(CO_3)_2$ precipitated around (or replacing) branches and twigs. The same tufa bed can be seen in many localities along the fault scarp, always underneath the stromatolites.

From the edge of the topographic scarp, after we have seen part of the bioherms down faulted towards the depocenter, we will follow a trail on the carbonate platform which surrounds the collapsed portion of the lake basin. As we move counterclockwise along the trail, towards the northeast, we will see marked changes in the deformation structures, as fault displacement gradually increases. Likewise, stromatolites in the bioherms will be better preserved; some of them grew around rock or wood fragments. In this area, at 20° 25'39.64"N, 101° 14' 47.13"W, there is a small bioherm developed around a fallen tree. Note that this particular bioherm lies a certain distance from the main scarp, and a subtle depositional dome does not surround it. Thus, its origin is slightly different from that of the bioherms located near the fault scarp.

Stop 5

Future main scarp (?) on the eastern side of the basin. Is the whole carbonate platform in the process of being destroyed by slope processes triggered by land subsidence?

As we move toward the northeast, we will see that total displacement on the incipiently developed fault system seen near the park increases. A notable graben is obvious southeast of the trail as we move closer to the site of Stop 5.

Beginning at this point (20°25'40.85"N, 101°14'44.78"W), a conspicuous normal fault scarp (Figure 20) and a series of rollover anticlines are clearly exposed on the calcareous platform, near the former shoreline. Vertical displacement is mostly concentrated at a single master fault; the fault plane of this master fault displays a paleosol underneath a thin cover of lake carbonates. Displacement in the master

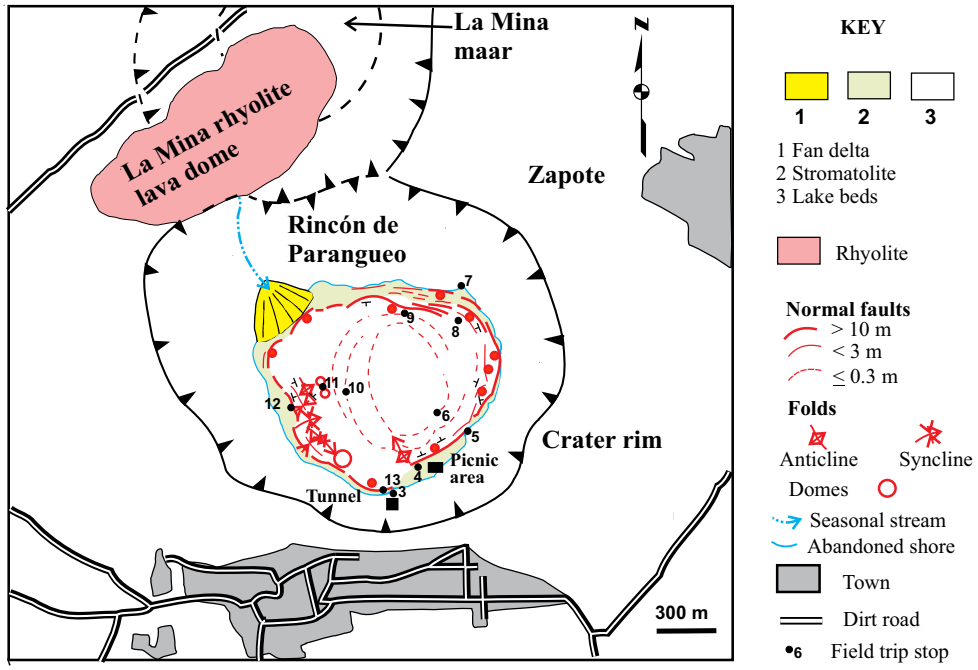

Figure 18. Structural sketch map of the bottom of the crater and location of Stops 3-13 Inferred faults or dissolution/collapse mini scarps (?) at the deepest part of the crater, near present day depocenter, are schematically depicted (modified after Aranda-Gómez *et al.*, 2013).

fault clearly increases toward the northeast. Just at the base of the master fault scarp is a small graben formed by secondary normal faults with antithetic movement with relation to the main fault (Figure 20).

As we follow the trail towards the northeast, we will see a gradual increase in the total displacement of the master fault, until it reaches 12 m. We speculate that in the future the "present-day main topographic scarp" will be completely destroyed by slope processes and the main scarp will be shifted closer to the former shoreline. Thus, the whole stromatolite platform will by destroyed by landslides. We view this near-shore fault system as evidence that deformation is propagating toward the crater´s wall.

At this point, it is worth to stress that the near-shore fault system must have a listric geometry (Figures 19 and 20), which causes the formation of rollover folds, as the hanging wall block deforms and rotates toward the fault. This anticline is highly asymmetric, as its northwestern limb is considerably steeper and longer than the southeastern limb (Figure 20). Likewise, this is a good place to mention some particularities of the deformation observed in Rincón de Parangueo lake sediments:

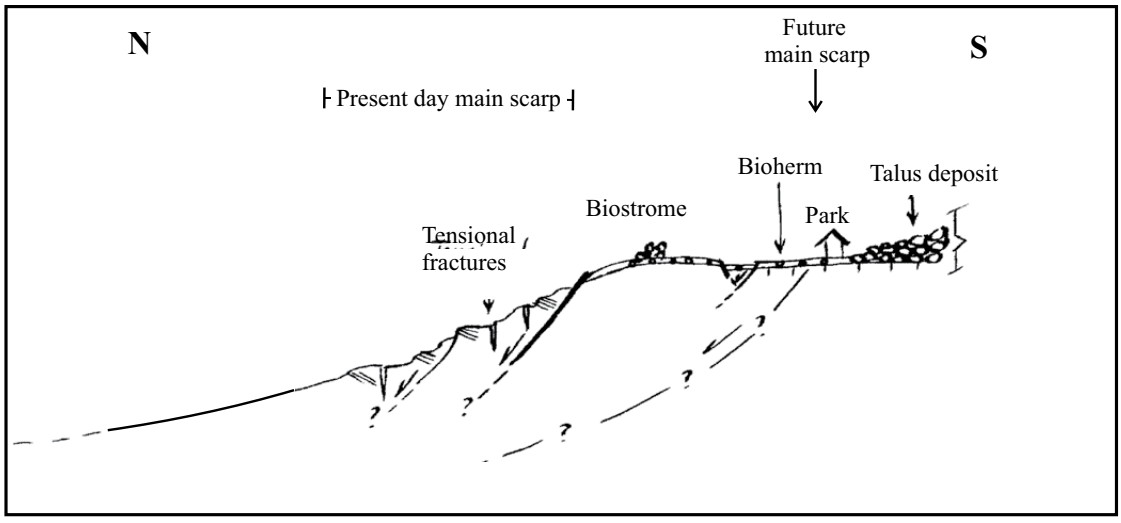

Figure 19. Schematic cross section near Stop 8. No scale (Aranda-Gómez *et al.*, 2013).

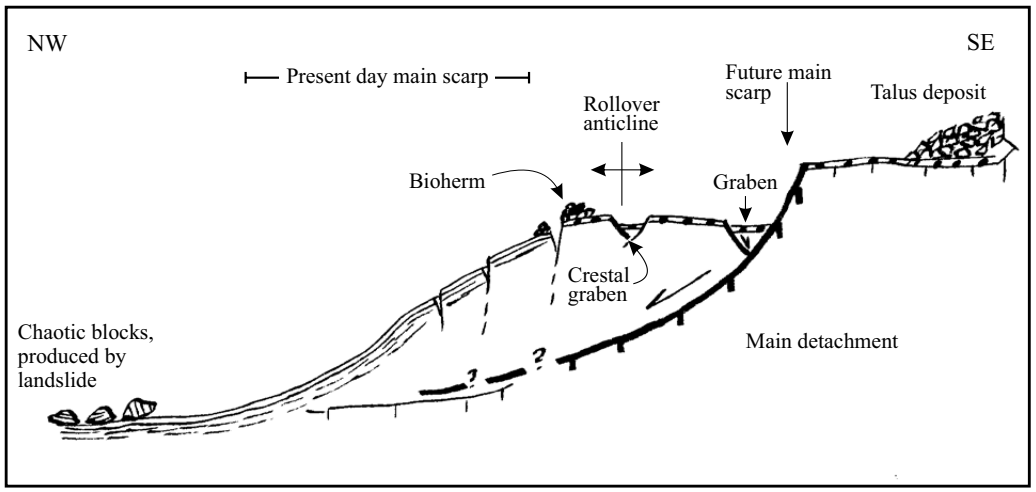

Figure 20. Schematic cross section near Stop 9. Landslide scar related to the megabreccia at the bottom of the scarp is not shown. No scale (modified from Aranda-Gómez *et al.*, 2013).

1. The lake sediments at the surface are dry and brittle, while the same sediments must be wet at depth and they have plastic behavior. As we will see along the traverse, these factors produce unusual combinations of structures.
2. Deformation at the near-shore fault system (mostly extension) is developing in unconfined sediments; the main fault scarp acts as a "free surface" (Figures 19 and 20). Most normal faults in the calcareous platform have a large horizontal throw, which may be as large as, or larger than, the vertical throw. Likewise, conspicuous sets of joints, one parallel to the shoreline and other perpendicular, also show large throws. One can interpret the hanging wall movement of the faults as a combination of down dip normal displacement and translation of material towards the depocenter of the basin. In the case of the open joints, there are two factors that operate simultaneously: one is the translation of material towards the depocenter, which favors the remarkable opening of the tensional fractures parallel to the lake shore. The other is lateral expansion of the platform in the areas located between landslide scars.
3. All the anticlines, rollover or ordinary compression folds, in the lake´s basin are crowned by crestal grabens (Figure 20). These structures, commonly with total vertical displacement between a few tens of centimeters to a couple of meters, reflect the formation of axial plane parallel tensional fractures formed during folding and the sediment translation towards the depocenter.
4. As a consequence of (1), some of the largest landslide deposits trigger the formation of mud domes, which may resemble endogenous lava domes or the first stages of formation of exogenous lava domes (see Stop 10 and Figure 25). Thus, it is common to find the landslide deposits deformed by domes developed by upward movement of mud caused by the weight of the landslide deposit.

Stop 6 (optional)
Landslide scar, landslide deposit, origin of microbreccias and gas bubbles in the water.

From (20°25'53.62"N,101°14' 38.58") we will leave the trail and walk towards the playa-lake shoreline (20°25'51.82"N, 101°14' 44.96"W). When we leave the trail we will be walking on a landslide scar (the surface may be somewhat wet and slippery; we recommend caution in order to avoid a fall).

Close to the base of the topographic scarp there is a megabreccia formed by large blocks (> 1m long) randomly oriented, which are interpreted as a part of a landslide deposit (Figure 20).

Near the shoreline of the playa-lake are plenty of examples of a microbreccia formed by randomly oriented, finely laminated, mudstone blocks, weakly cemented by mud. This microbreccia is interpreted as the product of the destruction of "desiccation columns" during past dry seasons and cementation with new mud during subsequent wet seasons. In this area there are blocks included in the microbreccia that show pre-landslide convoluted bedding. These structures are syn-sedimentary in origin (i.e. they predate lake desiccation) and they are probably related to underwater turbidity currents triggered by earthquakes while the perennial lake still existed.

On the surface of the water of the playa-lake is common to see isolated gas bubbles. Their origin is not yet clear to us, but in order to explain the presence of trona in the sediments, and following Earman *et al.* (2005) proposal, we speculate that the gases may be CO_2-rich and have a volcanic origin. However, during the rainy season,near the shoreline of the playa-lake we noticed the presence of floating rafts of algae (?) or bacteria surrounded by light brown foam, that suggests that some (or all?) the gas may be of organic origin. On the other hand, gas bubbles form small craters in thick evaporite crusts during the dry season

(Figure 21) when bacterial mats are not obvious. The formation of these craters indicates persistent bubbling thru a well localized conduit, which is more consistent with the idea of a volcanic source. We are planning to do gas sampling and analysis to ascertain the probable origin of the gas.

Stop 7
Composite landslide scarp on the northeastern side of the lake basin

We will go back to the trail and walk to 20°26'3.71"N, 101°14' 43.04"W, located at the NW end of a large composite landslide scar. We view this scarp, and the megabreccias accumulated at its base as formed by several coalescing landslides, probably with different ages. During our walk we will see complex deformation on the carbonate platform associated to the domain formed by normal faults with listric planes and associated rollover folds. In places there is more than one crestal graben. From this point we will climb down toward the base of the scarp, where several landslide deposits coalesce.

Stop 8
Young active faults cutting landslide deposit.

Near the base of the scarp there are several active normal faults cutting the landslide megabreccias. These structures demonstrate that deformation is still active in the region, as the faults are clearly cutting a deposit that post-dates the formation of the annular ring fault system. Likewise, these structures show that translation of the sediments occurs over very gently inclined slopes.

In this same area, clearly covered by several landslide deposits, there is a striking example of the unusual deformation in the relatively thin brittle cover underlain by ductile material. A series of tilted blocks outline the presence of a plunging synform, which was formed by the weight of the landslide deposit breaking the brittle mud (Figure 22). The end result of the process, sketched in the figure, is an array of tilted blocks that define a synform, but randomly oriented blocks of the landslide deposit occupy the central part of the structure.

Stop 9
Abandoned coastlines formed during desiccation and a large collapse feature, probably caused by evaporite dissolution at depth

As we move from the synform towards the large collapse feature, we will pass an area (20°26'1.38"N, 101° 14' 51.10"W) where several roughly parallel mini-scarps, less than 50 cm high, are exposed.

We interpret these mini-scarps (Figure 23) as abandoned coastlines formed as the crater-lake desiccated. One possible interpretation about the origin of the mini-scarps is that they were formed by wave action. However, we have noticed that even in the days with very strong winds inside the crater, the formation of waves in the very shallow water of the playa-lake is nil. An alternative interpretation of the origin of these mini-scarps is that they are collapse features formed at the end of the dry season at the shore of the playa-lake. We have noticed a striking difference in the morphology of the coastline during the rainy season and the dry season (Figure 24a). The water-sediment contact in the wet season is not a clear step as it is during the dry season (Figure 24b).

At 20°26'2.37"N, 101° 14 '53.34"W is exposed a large (80 x 12 m), shallow (< 1 m) collapse feature. It is locate just at the break of the slope of the main scarp, and in map view, it has the shape of two coalescing crescents. The collapse feature has an asymmetric form as the wall located near the main scarp

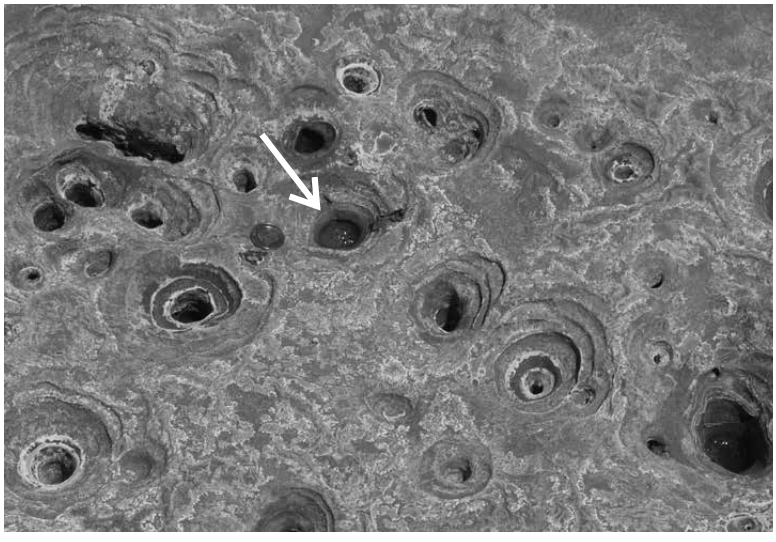

Figure 21. Thick crust of evaporite formed during the dry season of 2009. It shows small craters formed by gas bubbling thru the water (arrow). These craters suggest that gas was continuously expelled thru conduits that acted during time periods of days or weeks. Therefore, it seems that gas exsolution is not a diffuse process, as it would be expected if bacteria formed it. Note coin near the arrow as a scale (Aranda-Gómez *et al.*, 2013).

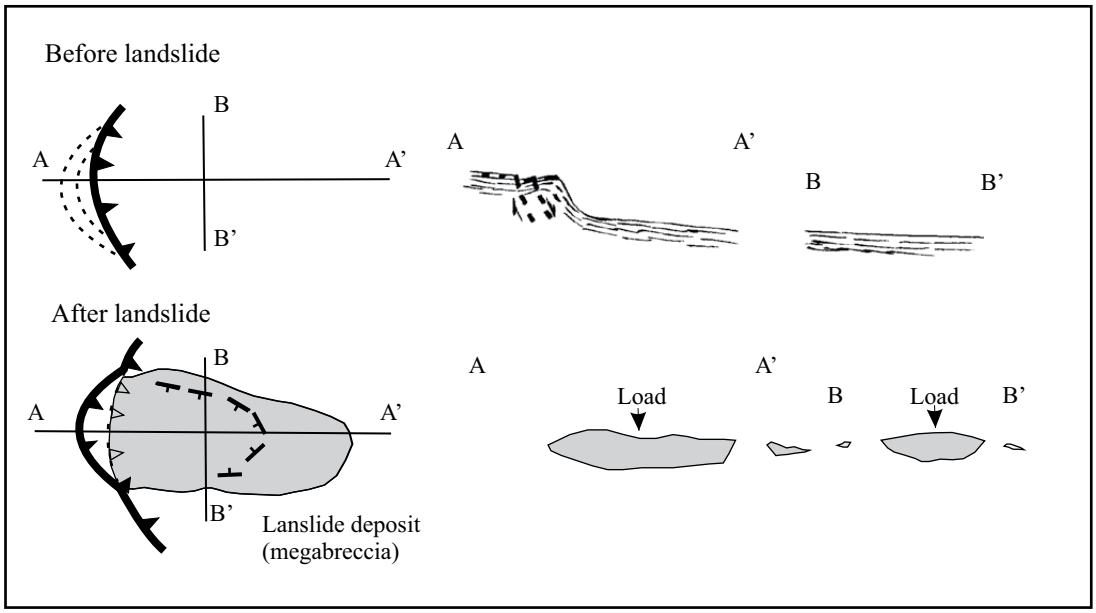

Figure 22. Formation of the "load synform" associated to a landslide deposit. This cartoon shows a possible mechanism for the development of the set of inclined blocks that appear to define a plunging syncline in the landslide deposit exposed in Stop 8. See text for discussion.

is higher (1 m) than the wall closer to the depocenter (< 50 cm). The bottom of the collapsed area is a flat surface, except near the walls where a series of tilted blocks occur. These blocks dip towards the walls that limit the collapsed area.

Stop 10
Mud-injection mini-dome cluster. An example of endogenous and quasi exogenous dome formation

From the collapse feature we will walk toward a dome chain located at the base of the domain where detachment faults appear to be flat surfaces. Approximately 100 m before we arrive to the dome chain we will find a small cluster of mini-domes.

These tiny domes (3 m in diameter and < 1 m high), exposed at 20°25'49.15"N, 101° 15' 3.20"W, are a good example of two end members of this kind of structures. In Figure 25, the dome on the left the structure has an aspect ratio of 3:1 and its core is occupied by structureless mud with a characteristic "pop corn" texture, while its flanks display steeply inclined, finely laminated, mudstone. The dome on the right has a larger aspect ratio (> 6:1) and lacks the structureless core. Attitude of the laminations in the mud clearly outline this last structure and it displays a clear star-shaped pattern of fractures radiating from its center. Note that there is no clear evidence of mud extrusion as in the neighboring dome.

The larger domes that we will see in Stop 11 display both features as they have two fracture patterns, one concentric and the other radial, and it is common to find mud with pop corn texture both at their apex and in the concentric fractures distributed throughout the structure.

Figure 23. Mini-scarp exposed in the area north of the playa-lake (Stop 9). These geomorphic features probably mark a previous coastline. They were probably formed by collapse (see Figure 24).

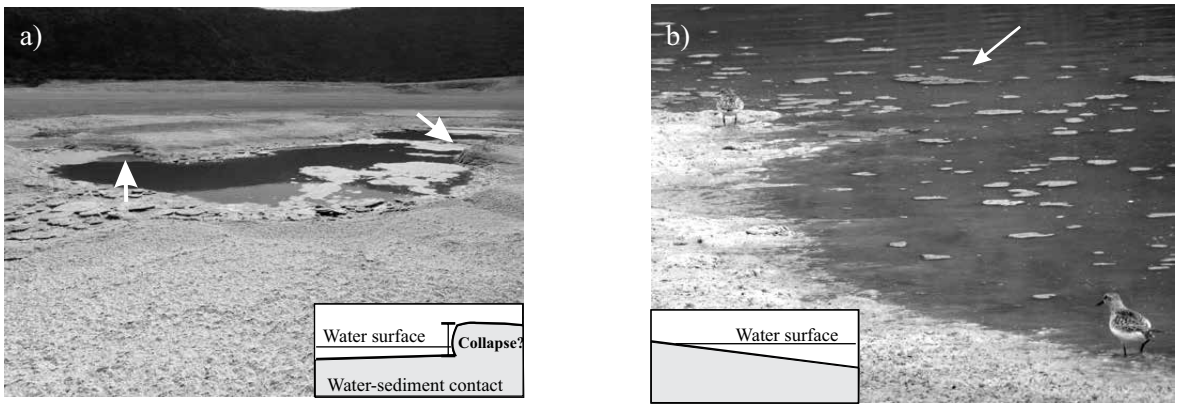

Figure 24. Contrasting morphologies of the coastline during the dry (a) and wet season (b). Insets attached to both photographs depict the sediment-water contact. Note that during the dry season the water is partially covered by a crust of evaporite, and the water-sediment contact is a clear step shown by the arrows. During the wet season (b) evaporites are dissolved and the water have floating bacterial mats (arrow).

Stop 11
Complex deformation associated with a flat detachment faults. Formation of a chain of mid-size mud domes and a syncline at the base of an attenuated topographic scarp

Once that we reach 20°25'49.69"N, 101° 15' 7.64"W we will be at the top of an elongated hill, which is parallel to the topographic scarp.

At this site, it is obvious that the hill is formed by a series of at least six domes. Between this site and the monocline exposed on the attenuated topographic scarp there is a syncline (Figure 26). Looking towards the west, we will see that both sets of tensional fractures exposed on the scarp, display large horizontal throws. The disposition of the blocks on the scarp, somewhat resembles tiers of concentric seats in an amphitheater.

Stop 12
Flat detachment cropping out at the edge of the attenuated topographic scarp

We will walk across the syncline located between Stops 11 and 12. We will climb the attenuated scarp walking inside some of the open fractures. Climbing the scarp standing on top of the blocks is more difficult as some tensional fractures may have a horizontal throw ≥ 2 m

When we reach 20°25'47.92" N, 101°15'10.66" W, we will find a large stromatolite bioherm clearly cut by a nearly vertical normal fault, with a vertical throw of approximately 2 m. Here is obvious that the horizontal throw may be as large as the vertical throw. This array of structures (domes + folds + tier-like blocks + nearly vertical normal fault) and the absence of rollover folds, makes us believe that the fault surface must be a gently inclined, flat plane similar to that shown in Figure 26. Note that in this interpretation the blocks sliding down slope in the scarp combine the work similar to that of a bulldozer with the effect of the added weight of the moving material over ductile mud at depth. The end result is a deformation, which propagates approximately 250 m away from the site where the fault crops out.

Stop 13
Spring deposit (?) Is the location of the bioherms and main fault scarp controlled by the buried diatreme-country rock contact?

On the way back to the tunnel entrance, we will follow a trail that surrounds an area centered around 20° 25' 37.65"N, 101° 14' 58.05"W where the calcareous platform has been completely destroyed by landslides.

From the trail we can see several interesting features:

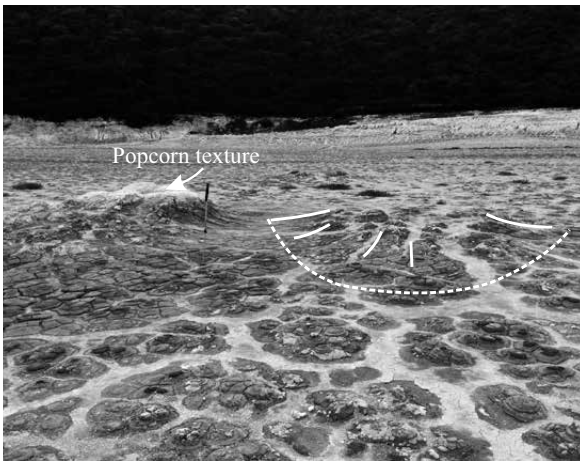

Figure 25. Contrasting morphologies of exogenous (left) and endogenous mini-domes. Presence of endogenous mini-domes can be detected by fractures with a characteristic radial pattern (not shown in this figure).

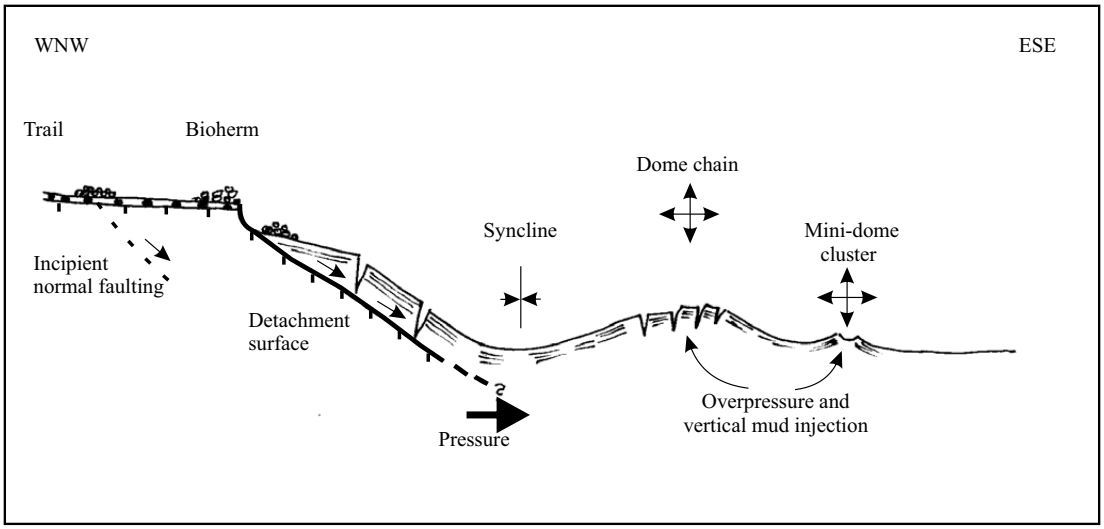

Figure 26. Schematic cross section between Stops 10 thru 12. Note the shape of the detachment surface near the western side of the section and the attenuated morphology of the scarp. No rollover folds have been documented in this structural domain. No scale (Modified after Aranda-Gómez *et al.*, 2013).

1. The largest mud dome in the basin (20°25'42.43"N, 101°15'4.01"W) has a basal diameter of 50 m and is 15 m high.
2. Southeast of the largest dome there is another dome with a conspicuous radial fracture pattern, which resembles a star.
3. The area around 20° 25' 37.65"N, 101° 14' 58.05"W is structurally complex. There are many large blocks, randomly oriented, probably associated to several landslides deposits that coalesce in this area. The weight of the landslide deposits has caused mud removilization and formation of a large dome complex in the area, which is in part obscured by the chaotic disposition of the blocks in the megabreccia.

Our final stop in this field trip is at 20°25'34.80"N, 101°14' 55.49"W where a small chimney-like feature (Figure 27a) is exposed. It resembles a small geyserite basin formed around hot springs (Figure 27b). We believe this is a key feature to understand the presence of the bioherm clusters along the fault scarp (Figure 8). We speculate that bioherms were constructed near hot springs located along the buried diatreme – country rock contact. This same feature also played an important role in the nucleation of the subsidence – related normal faults and the formation of the forced extensional fold shown in Figure 8. There are several of these features exposed along the fault scarp located between Stops 12 and 13. Although the lithology of these features is somewhat similar to a regular stromatolite bioherm in Parangueo, we note that a nearly vertical array of structures, which appear to be absent in the other bioherms seen elsewhere in the basin. We believe that here, where the carbonate platform is partially to completely destroyed, we are looking a deeper level of exposure in the core of a bioherm cluster.

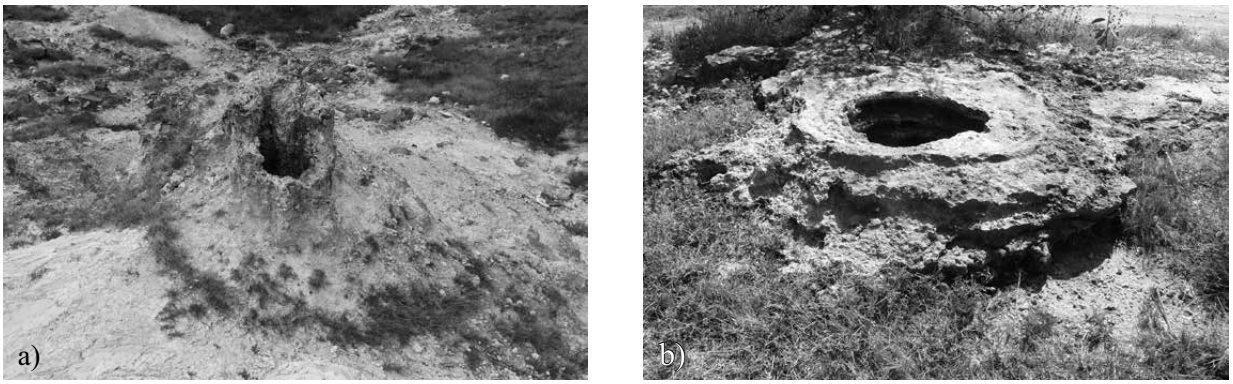

Figure 27. (a) Chimney-like hot spring (?) structure exposed on the main fault scarp. (a) This structure, found at the edge of the main fault scarp, is somewhat similar to sinter deposits found at some hot springs. (b) Sinter deposit around a hot spring near Querétaro. Here the initial precipitate is $CaCO_3$, which is later replaced by cryptocrystalline silica.

REFERENCES

Alaniz-Alvarez, S.A., Nieto-Samaniego, A.F. *et al.*, 2002, El sistema de fallas Taxco-San Miguel Allende: implicaciones en la deformación post-eocénica del centro de México: Boletín de la Sociedad Geológica Mexicana, v. LV(1), p. 12-29.

Aranda-Gómez, J.J.,Carrasco-Nuñez, G., *et al.*, 2010a, The maar volcanoes of the Valle de Santiago region (Guanajuato, México): a record of water-molten rock interaction: Water Rock Interaction - 13, Guanajuato, Gto. México, 25p.

Aranda-Gómez, J.J., Levresse, G., *et al.*, 2010b, Active subsidence at the bottom of a recently desiccated crater-lake and its environmental impact: Rincón de Parangueo, Guanajuato, México: Field trip guidebook: Eight International Symposium on Land Subsidence, Querétaro, Qro., México, Universidad Nacional Autónoma de México, Centro de Geociencias, 48 pp.

Aranda-Gómez, J.J., Chacón-Baca, E., Charles-Polo, M., Solorio-Munguía, J.G., Vega-González, M., Moreno-Arredondo, A., and Origel-Gutiérrez, G., 2009, Collapse structures at the bottom of a recently desiccated maar lake: Rincón de Parangueo maar, Valle de Santiago, México, *in* IAVCEI, 3rd International Maar Conference: Malargüe, Argentina, p. 3-4.

Aranda-Gómez, J.J., Levresse, G., *et al.*, 2013, Active sinking at the bottom of the Rincón de Parangueo Maar (Guanajuato, México) and its probable relation withs ubsidence faults at Salamanca and Celaya: Boletín de la Sociedad Geológica Mexicana v. 65(1), p.169-188.

Aranda-Gómez, J.J., Luhr, J.F., *et al.*, 2007, Late Cenozoic intraplate-type volcanism in central and northern México: A review, *in* S. A. Alaniz-Álvarez and A. F. Nieto-Samaniego eds., Geology of Mexico: Celebrating the Centenary of the Geological Society of México, Boulder, CO, Geological Society of America. Special Paper, v. 422**,** p.93-128.

Aranda-Gómez, J.J., Cerca, M., Rocha-Treviño, L., Pacheco-Martínez, J., Levresse, G., Ramos-Leal, J.A., Yutsis, V., and Arzate-Flores, J., 2014a, Structural analysis of subsidence-related deformation at the bottom of Rincón de Parangueo maar, México, Abstract volume IAVCEI – 5IMC, Querétaro, México, p. 143-144.

Aranda-Gómez, J.J., Luhr, J.F., Housh, T.B., and Carranza-Castañeda, O., 2014b, The Yuriria – Valle de Santiago – Irapuato maar lineament (Guanajuato, México); an overview: Abstract volume IAVCEI – 5IMC, Querétaro, México, 41-42.

Aranda-Gómez, J.J., Rocha-Treviño, L., and Pacheco-Martínez, J., 2014c, Detailed geologic map of the bottom of Rincón de Parangueo maar, México: evidence of active subsidence: Abstract volume IAVCEI – 5IMC, Querétaro, México, p. 141-142.

Armienta, M. A., Vilaclara, G., De la Cruz-Reyna, S., Ramos, S., Ceniceros, N., Cruz, O., Aguayo, A., and Arcega-Cabrera, F., 2008, Water chemistry of lakes related to active and inactive Mexican volcanoes: Journal of Volcanology and Geotthermal Research, 178, 249-258.

Arzate, J.A., Aguirre-Díaz, G.J. *et al.*, 1999, Mediciones geofísicas aplicadas al estudio de la falla Tarimoro-San Miguel Allende (SMA); una posible discontinuidad mayor en el basamento, GEOS, 19 (4), 237.

Avila-Olivera, J. A., and Garduño-Monroy, V.H., 2008, A GPR study of subsidence-creep-fault processes in Morelia, Michoacán, México: Engineering Geology, v. 100, p. 69-81.

Ban, M., T. Hasenaka, *et al.*, 1992, K-Ar ages of lavas from shield volcanoes in the Michoacán-Guanajuato volcanic field: Geofísica Internacional, 3(4), 467-474.

Blatter, D. L. and Hammersley, L., 2010, Impact of the Orozco Fracture Zone on the central Mexican Volcanic Belt: Journal of Volcanology and Geothermal Research, doi:10.1016/j.jvolgeores.2009.08.002.

Borja-Ortíz, R.I. and Rodríguez C., R., 2004, Aquifer vulnerability changes due to faults and river beds in Salamanca, Guanajuato, Mexico: Geofísica Internacional, 43 (4), 623-628.

Brown, R. J., Branney, M. J., Maher, C., and Dávila-Harris, P., 2010, Origin of accretionary lapilli within ground-hugging density currents: evidence from pyroclastic couplets on Tenerife: GSA Bulletin, 122 (1-2), 305-320.

Closson, D., 2004, Structural control of sinkholes and subsidence hazards along the Jordanian Dead Sea coast: Environmental Geology, 47(2), 290-301.

Closson, D., Karaki, N.A., Klinger, Y., and Hussein, M.J., 2005, Subsidence and sinkhole hazard assessment in the southern Dead Sea area, Jordan: Pure Appl. Geophys, 162, 221-248.

Connor, C.B., 1990, Cinder cone clustering in the TransMexican volcanic belt: Implications for structural and petrological models: Journal of Geophysical Research, (95), 19395-19405.

Earman, S., Phillips, F.M., and McPherson, B.J.O.L., 2005, The role of "excess" CO_2 in the formation of trona deposits, Applied Geochemistry, 20, 2217-2232.

Escolero-Fuentes, O.A. and Alcocer-Durand, J., 2004, Desecación de los lagos cráter del Valle de Santiago, Guanajuato, *in* Jiménez, B., Marín, L., Morán, D., Escolero, O., and Alcocer, J., (eds.), El agua en México vista desde la Academia, México, D.F., Academia Mexicana de Ciencias, p. 99- 116.

Hasenaka, T., 1992a, Contrasting volcanism in the Michoacán-Guanajuato volcanic field, central Mexico, *in* Aoki, K.I., (ed.) Subduction volcanism and tectonics of western Mexican Volcanic Belt: Sendai, Japan, the Faculty of Science, Tohoku University, 142-162.

Hasenaka, T., 1992b, Size, distribution and magma output rate for shield volcanoes of the Michoacán-Guanajuato volcanic field, central Mexico, *in* Aoki, K.I. (ed.) Subduction volcanism and tectonics of western Mexican Volcanic Belt: Sendai, Japan, the Faculty of Science, Tohoku University, 115-141.

Hasenaka, T., and Carmichael, I.S.E., 1985, The cinder cones of the Michoacan-Guanajuato, central Mexico: their age, volume, and distribution, and magma discharge rate, Journal of Volcanology and Geothermal Research, 25, 104-124.

Hernández, H., 2007, Problemática del acuífero Irapuato-Valle de Santiago, acciones que se están realizando para inducer el manejo sustentable del agua: Memoria del Taller de Análisis de Estrategias para la Gestión de Acuíferos en zonas agrícolas: Instituto Mexicano de Tecnología del Agua , 19p.

Highland, L., 2004, Landslides types and processes, U.S. Geological Survey Fact sheet 2004-3072. 1-4, http://pbs.usgs.gov/fs/2004/3072/

Johnson, C. A., and Harrison, C. G. A., 1990, Neotectonics in central Mexico: Phys. Earth Planet. Int., v. 64, p. 187-210.

Kienel, U., Wulf Bowen, S., Byrne, R., Park, J., Böhnel, H., Dulski, P., Luhr, J. F., Siebert, L., Haug, G.H., and Negendank, J.F.W., 2009, First lacustrine varve chronologies from Mexico: impact of droughts, ENSO and human activity since AD 1840 as recorded in maar sediments from Valle de Santiago: Journal of Paleolimnology, DOI 10.1007/s10933-009-9307-x.

Leake, S.A., 2010, Land subsidence from ground-water pumping: http://geochange.er.usgs.gov/sw/changes/anthropogenic/subside/

Lorenz, V., 2003, Maar-diatreme volcanoes, their formation, and their setting in hard-rock or soft-rock environments: Geolines, 15, 72-83.

Luhr, J.F., Kimberly, P., Siebert, L., Aranda-Gómez, J.J., Housh, T.B., and Kysar, G., 2006, México's Quaternary volcanic rocks: Insights from the MEXPET petrological and geochemical database: Geological Society of America Special Paper, 402, 1-44.

Martínez- Reyes, J. and Nieto-Samaniego, A.F., 1992, Efectos geológicos de la tectónica reciente en la parte central de México: Universidad Nacional Autónoma de México, Instituto de Geología, Revista, 9, 33-50.

Molina-Garza, R.S. and Urrutia-Fucugauchi, J., 1993, Deep crustal structure of central Mexico derived from interpretation of Bouger gravity anomaly: Journal of Geodynamics, v. 17, p. 181-201.

Murphy, G.P., 1986, The chronology, pyroclastic stratigraphy, and petrology of the Valle de Santiago maar field, central Mexico: University of California, Berkeley, Master of Science thesis, 55 pp.

Nakamura, K., 1977, Volcanoes as possible indicators of tectonic stress orientation- principle and proposal: Journal of Volcanology and Geothermal Research, v. 2, p. 1-16.

Ordóñez, E., 1900, Les volcans du Valle de Santiago: Memorias de la Sociedad Científica Antonio Alzate (México), XIV, 299-326.

Orozco, F. and Madinaveitia, A., 1941, Estudio químico de los lagos alcalinos, An. Inst. Biol. Univ. Nal. Autón. México, 12, 429-438.

Ortega-Gutiérrez, F., Gómez-Tuena, A., *et al.*, 2014, Petrology and geochemistry of the Valle de Santiago lower-crustal xenoliths: Young tectonothermal processes beneath the central Trans-Mexican volcanic belt: Lithosphere, 1-27.

Pacheco-Martínez, J., 2007, Modelo de subsidencia del Valle de Querétaro y predicción de agrietamientos superficiales: Universidad Nacional Autónoma de México, PhD thesis, 225 pp.

Pardo, M. and Suárez, G., 1995, Shape of the subducted Rivera and Cocos plates in southern Mexico: seismic and tectonic implications: Journal of Geophysical Research, 100, 12357-12373.

Righter, K. and I. S. E. Carmichael, 1993, Mega-xenocrysts in alkali basalts: fragments of disrupted mantle assemblages: American Mineralogist, 78, 1230-1245.

Rincón, N., 2005, Estratigrafía del cráter de explosión Hoya La Alberca: Instituto Tecnológico de Ciudad Madero, Geological Eng. Thesis, 78 pp.

Urrutia-Fucugauchi, J., A. M. Soler-Arrechalde, and J. H. Flores-Ruiz, 1995, Tectonics and volcanism in central Mexico -influence of pre-Neogene tectonics in the plate subduction-magmatic arc system: Geological Society of America, Abstracts with programs, 27, A189.

Walter, M. R., 1976, Stromatolites: Developments in Sedimentology 20, 790 pp.

Whitjack, M.O., Olson, J., Peterson. E., 1990, Experimental models of forced extensional folds: AAPG Bulletin, 74, 1038-1054.

Zimanowsky, B., Bütner, R., Lorenz, V., 1997, Premixing of magma and water in MFCI experiments: Bulletin of Volcanology, 58, 491-495.

§

We acknowledge our sponsors for their support to this meeting:

Centro de Geociencias
Universidad Nacional Autónoma de México
Querétaro, Mexico, November 2014